Published in final edited form as:

Traffic. 2020 June ; 21(6): 430–450. doi:10.1111/tra.12731.

ESCRT-dependent protein sorting is required for the viability of yeast clathrin-mediated endocytosis mutants

Kyle Hoban[1], **Samantha Y. Lux**[1], **Joanna Poprawski**[1], **Yorke Zhang**[1], **James Shepherdson**[1], **Pedro G. Castiñeira**[1], **Sanjana Pesari**[1], **Tony Yao**[1], **Derek C. Prosser**[2], **Carolyn Norris**[1], **Beverly Wendland**[1]

[1]Department of Biology, Johns Hopkins University, Baltimore, Maryland

[2]Department of Biology, Virginia Commonwealth University, Richmond, Virginia

Abstract

Endocytosis regulates many processes, including signaling pathways, nutrient uptake, and protein turnover. During clathrin-mediated endocytosis (CME), adaptors bind to cytoplasmic regions of transmembrane cargo proteins, and many endocytic adaptors are also directly involved in the recruitment of clathrin. This clathrin-associated sorting protein family includes the yeast epsins, Ent1/2, and AP180/PICALM homologs, Yap1801/2. Mutant strains lacking these four adaptors, but expressing an epsin N-terminal homology (ENTH) domain necessary for viability (4Δ+ENTH), exhibit endocytic defects, such as cargo accumulation at the plasma membrane (PM). This CME-deficient strain provides a sensitized background ideal for revealing cellular components that interact with clathrin adaptors. We performed a mutagenic screen to identify alleles that are lethal in 4Δ+ENTH cells using a colony-sectoring reporter assay. After isolating candidate synthetic lethal genes by complementation, we confirmed that mutations in *VPS4* led to inviability of a 4Δ+ENTH strain. Vps4 mediates the final step of endosomal sorting complex required for transport (ESCRT)-dependent trafficking, and we found that multiple ESCRTs are also essential in 4Δ+ENTH cells, including Snf7, Snf8 and Vps36. Deletion of *VPS4* from an *end3*Δ strain, another CME mutant, similarly resulted in inviability, and upregulation of a clathrin-independent endocytosis pathway rescued 4Δ+ENTH *vps4*Δ cells. Loss of Vps4 from an otherwise wild-type background caused multiple cargoes to accumulate at the PM because of an increase in Rcy1-dependent recycling of internalized protein to the cell surface. Additionally, *vps4*Δ *rcy1*Δ mutants exhibited deleterious growth phenotypes. Together, our findings reveal

Correspondence: Beverly Wendland, Department of Biology, Johns Hopkins University, Baltimore, MD 21218. bwendland@jhu.edu.
Present address
Samantha Y. Lux, Skirball Institute of Biomolecular Medicine, New York University School of Medicine, New York, NY 10016
Joanna Poprawski, The Scripps Research Institute, Jupiter, FL 33458
Yorke Zhang, Synthorx, Inc., La Jolla, CA 92037
James Shepherdson, Washington University School of Medicine, St. Louis, MO 63110

CONFLICT OF INTEREST

The authors certify that they have no affiliations with or involvement in any organization or entity with any financial or non-financial interest in the subject matter or materials discussed in this manuscript.

Peer Review

The peer review history for this article is available at https://publons.com/publon/10.1111/tra.12731/

SUPPORTING INFORMATION

Additional supporting information may be found online in the Supporting Information section at the end of this article.

previously unappreciated effects of disrupted ESCRT-dependent trafficking on endocytic recycling and the PM.

Keywords

clathrin-independent endocytosis; clathrin-mediated endocytosis; endosomal sorting complex required for transport; epsin N-terminal homology domain; intralumenal vesicle; multivesicular body; plasma membrane; vacuolar protein sorting

1 | INTRODUCTION

In addition to providing a barrier that isolates the cytoplasm from variable conditions in extracellular spaces, the plasma membrane (PM) contains a variety of proteins with different functions, including ion channels, transporters, enzymes, and receptors. In response to fluctuating conditions in the environment, the makeup of the PM must be continuously adjusted for optimal cellular physiology. One mechanism by which the composition of this surface membrane is regulated is endocytosis, a process that generates intracellular vesicles to remove material from the PM. Proteins that are recognized and internalized by the endocytic machinery are referred to as cargoes. The main pathway by which cargoes are moved from the cell surface to the cell interior is clathrin-mediated endocytosis (CME), a membrane trafficking route in which dozens of proteins coordinate to form clathrin-coated vesicles within cells.

In the first phase of CME, members of the early coat localize to nascent sites of endocytosis where they facilitate cargo recruitment and clathrin assembly.[1,2] These early-arriving components then recruit late coat proteins that, in turn, regulate the function of actin remodelers. Actin-polymerizing factors generate force at the PM, contributing to membrane curvature and the formation of a clathrin-coated pit. Scission factors such as dynamin and amphiphysin then constrict the neck of the pit and allow for release of an endocytic vesicle into the cytoplasm.[1–3] The CME pathway is highly conserved through evolution, with most components of the mammalian CME machinery sharing homology with at least one budding yeast (*Saccharomyces cerevisiae*) protein associated with endocytosis.[3–5] After leaving the PM, endocytosed cargo is delivered along a series of compartments within the cytoplasm that make up the endocytic pathway.

The first destination of an endocytic vesicle is the early endosome, an organelle that sorts cargo for delivery to multiple potential locations within the cell. Some cargoes undergo endocytic recycling and are returned to the PM via delivery to recycling endosomes,[6–9] while other proteins remain at the early endosome for delivery to the late endosome. Recent evidence suggests that, unlike other eukaryotic species, budding yeast lack early endosomes.[10] In place of these organelles, the *trans*-Golgi network may be the initial target of endocytosed material, which then either recycles proteins or transfers them to the yeast equivalent of the late endosome. Late endosomes possess cargo-containing intralumenal vesicles (ILVs) that are generated through the invagination and scission of endosomal membranes.[11–13] These vesicle-laden endosomes are present in both yeast and mammalian cells and are also referred to as multivesicular bodies (MVBs). The formation of ILVs in this

MVB pathway is mediated by endosomal sorting complex required for transport (ESCRT) proteins. In the final step along the endocytic route, late endosomes fuse with highly acidic organelles called vacuoles, the yeast equivalent of lysosomes in mammalian cells,[14] for degradation of the endosomal contents.

Adaptor proteins are among the earliest arriving factors of the CME early coat. Endocytic adaptors bind to cargoes, lipids within the PM, and other endocytic components, including clathrin itself.[15–17] Among the CME adaptors in budding yeast are four related proteins: the yeast epsins, Ent1 and Ent2, and the AP180/PICALM homologs, Yap1801 and Yap1802.[18,19] All of these adaptors possess C-terminal clathrin-binding motifs, as well as multiple Asn-Pro-Phe (NPF) tripeptide motifs, which interact with Eps15-homology (EH) domains found in other CME proteins.[20–22] Yap1801 and Yap1802 each contain an AP180 N-terminal homology (ANTH) domain, while the epsins possess a similar epsin N-terminal homology (ENTH) domain. ENTH and ANTH domains both bind to PtdIns(4,5)P_2,[23,24] and Ent1 and Ent2 additionally contain ubiquitin-interacting motifs that participate in cargo recognition.[18] The nonessential *YAP1801* and *YAP1802* genes can be deleted individually or together. In contrast, yeast lacking both *ENT1* and *ENT2* are inviable; this type of negative genetic interaction is known as synthetic lethality. However, retention of a single copy of the ENTH domain-encoding fragment of either gene (2Δ+ENTH) is sufficient for viability.[18,25]

One protein cargo that undergoes endocytosis in yeast is Ste3, the *MATα* cell receptor for **a**-factor mating pheromones. In the absence of **a**-factor, Ste3 expressed in a wild-type (WT) strain is delivered to the PM, constitutively endocytosed, and delivered to the vacuole for degradation.[26] In cells lacking both Ent1 and Ent2 but expressing a viability-supporting ENTH domain, endocytosis remains largely unaltered compared to WT yeast. However, additional deletion of *YAP1801* and *YAP1802* from the epsin double mutant background (4Δ+ENTH) leads to nonspecific cargo accumulation at the PM, as well as a temperature-sensitive growth phenotype.[19,27,28] For example, while Ste3 localizes almost exclusively to the vacuole in WT or 2Δ+ENTH cells, this receptor accumulates significantly at the PM in 4Δ+ENTH adaptor mutants.

The 4Δ+ENTH strain provides a unique tool for identifying factors that cooperate, or function in parallel with, endocytic adaptor proteins. In this study, we performed a random, chemical mutagenesis screen using a colony-sectoring reporter strain to identify genes that become essential in the 4Δ+ENTH background. We investigate a lethal interaction between this endocytosis mutant and the loss of functional Vps4, an ATPase best known for its role in ESCRT complex disassembly, which allows for vesicle scission and release into the lumen of MVBs.[29–31] We demonstrate that ESCRT-dependent trafficking is required for the viability of 4Δ+ENTH cells, as well as the viability of another CME mutant that lacks End3. Our data also indicate that cargo accumulation within the prevacuolar structures that form in MVB pathway mutants leads to the redirection of endocytosed material into the Rcy1-dependent endocytic recycling pathway. Together, these findings reveal a previously unappreciated connection between CME and ESCRT-dependent trafficking.

2 | RESULTS

2.1 | Isolating lethal alleles in cells lacking clathrin-binding adaptors

To identify alleles that are lethal in the adaptor mutant background, we generated 4Δ+ENTH strains in which the *ENT1* locus was truncated by integrating a stop codon immediately after the ENTH domain (Table 2; BWY5678 and BWY5679). We then transformed these strains with a cover plasmid that contains a WT copy of the *ENT1* gene; reintroduction of full-length Ent1 alone is able to rescue known phenotypes associated with the 4Δ+ENTH genotype.[19] To simplify the task of distinguishing synthetic lethal mutants from those that remain viable without the full-length Ent1 vector, we utilized adenine biosynthesis mutations in a colony-sectoring assay that is similar to one described in Bender and Pringle, 1991.[32] In *ade2* mutants, the substrate for the Ade2 enzyme, aminoamidozole ribonucleotide (AIR), accumulates and causes the cells to acquire red pigmentation. However, the additional deletion of genes encoding products that act upstream of AIR formation, such as *ADE8*, prevents its production and results in colonies that are white.[33–35]

We deleted both *ADE2* and *ADE8* from the 4Δ+ENTH mutants while providing a copy of *ADE8* on the Ent1 cover plasmid. Thus, our 4Δ+ENTH *ade2*Δ *ade8*Δ+Ent1 [Ade8] reporter cells produce red colonies when grown on minimal medium that selects for maintenance of the vector (Figure 1A). After mutagenesis, cells in which no synthetic lethal mutation is introduced will not require the full-length Ent1 plasmid for viability; therefore, these cells will randomly lose the cover plasmid during cell division and form colonies with white sectors when grown on nonselective medium (Figure 1A; B, left). In contrast, cells that do acquire a synthetic lethal mutation will be inviable without the Ent1 [Ade8] plasmid and produce completely red, nonsectored colonies on rich medium (Figure 1B, right). These nonsectoring colonies are easily distinguished from those that do sector.

We treated the 4Δ+ENTH *ade2*Δ *ade8*Δ+Ent1 [Ade8] yeast of both mating types with ethyl methanesulfonate (EMS), a chemical that introduces point mutations into the genome. After mutagenesis, we allowed colonies to form on rich medium. Entirely red colonies were identified visually, and only cells that continued to be nonsectoring upon restreaking were selected for further analysis. To confirm that the nonsectoring phenotype was not because of a genomic integration of the Ent1 [Ade8] cover plasmid, which also contains the URA3 gene, we performed a plasmid shuffling experiment to exchange it with an Ent1 [Trp1] vector. To this end, we transformed nonsectoring cells with an Ent1 [Trp1] plasmid and grew the cells on medium containing 5-fluoroorotic acid (5-FOA), which selects against the *URA3*-containing cover plasmid.[36] We eliminated all strains for which the plasmid shuffle was unsuccessful. Next, we backcrossed the remaining mutants several times, mating each strain to the unmutagenized parent of opposite mating type and selecting the nonsectoring spores after tetrad dissection. This backcrossing procedure removed many of the background mutations introduced during EMS treatment that were unrelated to the allele causing inviability.

Backcrossing also allowed us to designate the synthetic lethal mutations as either dominant or recessive. Following the mating of each synthetic lethal mutant with the appropriate parental strain, those matings that produced nonsectoring diploids were classified as

dominant, whereas those that yielded sectoring diploids were categorized as recessive. We then mated each recessive mutant with every recessive strain of the opposite mating type to organize them into complementation groups, which are likely comprised of cells that have mutant alleles of the same gene. From this analysis, we were able to identify eight complementation groups with multiple members.

We next aimed to identify the alleles that are synthetic lethal in the 4Δ+ENTH background. We transformed representative mutants from each complementation group with a low-copy *TRP1* genomic library[37] and screened for cells that regained viability without the Ent1 cover plasmid by replica plating transformants onto medium containing 5-FOA, thereby selecting for loss of the Ent1 [Ade8 Ura3] vector (Figure S1A). Library plasmids were then isolated from cells confirmed to be growing without the original Ent1 vector. Because of the presence of plasmids containing *ENT1/2* or *YAP1801/2* in the genomic library, all of which are capable of rescuing the phenotypes associated with the 4Δ+ENTH mutant, the isolated library vectors were tested for the presence of these genes by PCR (Figure S1B). All rescuing vectors lacking the four adaptor-encoding genes were then sequenced to identify candidate genes for the causative allele.

2.2 | Many synthetic lethal mutants exhibit vacuolar protein sorting defects

From rescued complementation group 3 cells, we isolated two distinct library plasmids that contained an overlapping genomic interval. The three full-length genes present on both vectors encode proteins with unconfirmed functions, Ypr172w and Ypr174c, as well as Vps4 (Figure 2A). Vps4 is a conserved ATPase associated with diverse cellular activities (AAA) that allows for ESCRT-III complex disassembly and release of cargo-containing vesicles into the lumen of MVBs.[29–31] *VPS4* was the likely candidate for synthetic lethality in 4Δ+ENTH cells because of its function along the endocytic route, though it is mainly known to act at intracellular locations as opposed to at the PM.

Hydrolytic enzymes are normally delivered to the vacuolar lumen to aid in degradative processes, but *vps4* mutants aberrantly secrete vacuolar hydrolases into the extracellular environment.[31,38] To test for this phenotype, we utilized an assay in which cells are grown in direct contact with nitrocellulose, and the membrane is then probed for secreted carboxypeptidase Y (CPY), one such vacuolar enzyme. While WT, 4Δ+Ent1 and 4Δ+ENTH parental strains were negative for CPY secretion, synthetic lethal mutants from complementation group 3 strains, particularly 3α, secreted this hydrolase, similar to the *vps4*Δ positive control strains (Figure 2B). The signal from Group 3 mutants was far less robust than the *vps4*Δ controls; this is likely a result of the slower growth rate of the synthetic lethal mutants. We also tested representative strains from the other complementation groups, and both mutants from groups 2 to 5 were positive for CPY secretion as well, indicating that vacuolar protein sorting defects are a common phenotype of 4Δ+ENTH synthetic lethal mutants.

Because of positive results from the CPY assay, we also transformed these synthetic lethal strains with a plasmid expressing another degradative vacuolar enzyme, carboxypeptidase S (CPS), fused to green fluorescent protein (GFP) at its N-terminus. In WT cells, GFP-CPS is delivered to the lumen of vacuoles via the ESCRT pathway. However, in the

absence of Vps4, this protein remains at the limiting membrane of the vacuole and accumulates in cargo-dense, class E organelles named for the group of vacuolar protein sorting (*vps*) mutants in which they were first observed.[38,39] Upon imaging, GFP-CPS localized to the lumen of vacuoles in WT, 4Δ+Ent1 and 4Δ+ENTH cells, as expected (Figure 2C). In the *vps4*Δ strain, the fluorescent protein instead appeared at vacuole surfaces and adjacent prevacuolar compartments, consistent with findings from previous studies.[40] We also observed a class E *vps* phenotype in group 3 strains, which were rescued by genomic fragments containing *VPS4*. These defects are indicative of vacuolar protein sorting dysregulation and further suggested that *vps4* alleles were the causative, synthetic lethal mutations in these cells.

Representative mutants from other complementation groups also exhibited abnormal GFP-CPS localization (Figure 2C). Groups 2 and 5, which were positive for CPY secretion, also exhibited cargo accumulation in prevacuolar organelles as opposed to the vacuole lumen, confirming that cells in these complementation groups are class E *vps* mutants as well. Additionally, GFP-CPS was found in punctae within many cells from Groups 4 to 6 and at the vacuole membrane in those from Groups 7 to 8. The plasmid shuffling necessary for GFP-CPS imaging was unsuccessful for representative mutant 6**a** despite multiple attempts; it is possible that the Ent1 vector was incorporated into the genome of these cells after our initial confirmation tests but before subsequent analyses. Though we have been unable to identify the synthetic lethal gene in strains from other complementation groups thus far, the presence of class E *vps* phenotypes in strains from multiple complementation groups suggests that several individual components of the MVB pathway are essential in the CME-deficient 4Δ+ENTH strain.

2.3 | Vps4 mutations are lethal in combination with the 4Δ+ENTH background

We next sequenced the *VPS4* locus in these two representative strains from complementation group 3, and analysis of the results confirmed the presence of mutations in the *Vps4* coding sequence. One vps4 allele is the result of a frame-shift mutation within the eighth codon of *VPS4*, which introduces a stop codon at residue 11 (Figure 3A). The other is a D283V missense mutation. Though we have not yet confirmed that Vps4^{D283V} is expressed and folds properly, this aspartic acid is adjacent to a phosphate-sensing asparagine, residue 277, within the active site of the Vps4 large ATPase domain (Figure 3B), leaving open the possibility that the mutation inactivates this domain.

To verify the requirement for Vps4 in our CME-deficient cells, we deleted *VPS4* from the genome of a parental 4Δ+ENTH reporter strain. Cells without *VPS4* became dependent on the Ent1 cover plasmid for viability, producing colonies that were nonsectoring on rich medium (Figure 3C, top panel). The additional *vps4*Δ mutation also prevented growth of the 4Δ+ENTH yeast on medium containing 5-FOA, further demonstrating an acquired need for the Ent1[Ade8 Ura3] vector (Figure 3C, bottom panel). Furthermore, diploid cells formed by mating the 4Δ+ENTH *vps4*Δ+Ent1 [Ade8 Ura3] strain to a mutant from complementation group 3 were unable to sector on rich medium or grow in the presence of 5-FOA (Figure S1C). In contrast, these 4Δ+ENTH *vps4*Δ cells were complemented when mated to a parental strain, allowing diploid colonies to sector and grow on medium with

5-FOA. Intriguingly, high-throughput studies searching for synthetic genetic relationships between paired gene deletions in budding yeast previously identified negative interactions between the loss of Vps4 and several proteins involved in endocytosis, including Act1, Arp3, Las17, Rvs161 and Sla2,[41,42] supporting our identification of an interaction between *vps4* alleles and CME mutants using a classical genetics approach. Together, these findings confirm that Vps4 is essential for the viability of 4Δ+ENTH cells.

In addition to being synthetic lethal in 4Δ+ENTH cells, loss of Vps4 produces aberrant phenotypes even in a 4Δ+Ent1 strain that expresses the full-length *ENT1* gene. Budding yeast grow optimally at 30°C; like many endocytosis mutants, 4Δ+ENTH cells are temperature-sensitive and unable to grow at 37°C, but 4Δ+Ent1 cells can tolerate this higher temperature. However, the 4Δ+ENTH *vps4*Δ strain with an Ent1 cover plasmid was unable to grow at the restrictive temperature (Figure 3D). Thus, deletion of *VPS4* precludes the ability of full-length Ent1 to rescue the temperature-sensitivity associated with adaptor mutants and reveals that a negative genetic interaction exists between *vps4* alleles and an *ent2*Δ *yap1801*Δ *yap1802*Δ background.

2.4 | The MVB pathway is essential in 4Δ+ENTH cells

To test whether Vps4 ATPase activity is essential in 4Δ+ENTH mutants, we performed a plasmid-shuffling assay utilizing a dominant-negative allele, $VPS4^{E233Q}$, in which the large ATPase domain is inactive.[31] 4Δ+ENTH *vps4*Δ+Ent1 [Trp1] cells were transformed with a $VPS4^{E233Q}$-expressing vector and tested for the ability to grow without full-length Ent1 on medium containing 5-fluoroanthranilic acid (5-FAA), which is toxic to cells with Trp1 enzyme.[43] Untransformed 4Δ+ENTH *vps4*Δ strains with *ENT1* expressed from either a Ura3 or Trp1 plasmid were included as growth controls on the various media. The synthetic lethal mutants transformed with Ent1 [Ura3] were able to lose the original Ent1 [Trp1] vector and grow on medium with 5-FAA, as anticipated (Figure 4A). In contrast, 4Δ+ENTH *vps4*Δ+Ent1 [Trp1] cells expressing $VPS4^{E233Q}$ were inviable without the Ent1 plasmid and did not grow in the presence of 5-FAA, similar to the negative control cells transformed with an empty vector containing only *URA3*. Therefore, functioning of the Vps4 large ATPase domain is necessary for viability of 4Δ+ENTH cells. This experiment was performed in a *vps4*Δ strain because of the possibility that $Vps4^{E233Q}$ does not completely inhibit the activity of WT ATPase within the cell; in a similar experiment, a 4Δ+ENTH+Ent1 [Trp1] strain that retains a WT copy of *VPS4* was able to survive without full-length Ent1 when $Vps4^{E233Q}$ was present (Figure S3).

Having identified a genetic interaction with *vps4* alleles, we next tested the deletion of related genes for synthetic lethality in the adaptor mutant background. These were either additional Vps4 complex components, members of other classes of vacuolar protein sorting factors, or ESCRT genes. We constructed and analyzed mutants of non-ESCRT binding partners of Vps4: Ist1, Vfa1, and Vta1; ESCRT proteins: Hse1 (ESCRT-0), Vps28 (ESCRT-I), Snf8 and Vps36 (ESCRT-II), and Did2, Snf7, Vps20 and Vps24 (ESCRT-III); factors in other vacuolar protein sorting classes: Pep1 (class A), Vps5 and Vps41 (class B), Vps16 (class C), Vps3 and Pep12 (class D), and Pep8 (class F); and additional AAA enzymes not known to be involved in ESCRT-dependent trafficking: Yta6 and Sap1. Aside from the class

C *vps16*Δ strain, the deletion of all nonclass E *vps* genes produced cells that sectored and grew on medium counter-selective for the Ent1 cover plasmid, indicating that these are not synthetic lethal interactions (Figure S2; Table 1). In addition to these *vps* classes, genes encoding nonESCRT Vps4 binding partners and other AAA proteins were also nonessential in this context based on results of the growth assays.

Though not ESCRT- or Vps4-related, the class C *vps16*Δ cells did not sector or grow in the presence of 5-FOA, indicating a synthetic lethal interaction (Figure S2). Of note, the colonies from this strain were pink in color as opposed to the deeper red exhibited by other strains. The color difference is likely because of class C *vps* mutants lacking an organized vacuole, since the development of red pigmentation is dependent on the transport of AIR molecules into this organelle.[34] Loss of Vps16, like all other class C *vps* mutants, disrupts both the class C core vacuole/endosome tethering (CORVET) and homotypic fusion and protein sorting (HOPS) complexes.[44–46] Vps3 is a component of only the CORVET complex, which is necessary for the merging of endosomes, while Vps41 is a factor of the HOPS complex that mediates late endosome-vacuole and vacuole-vacuole fusion.[45,46] Neither gene deletion was lethal in the 4Δ+ENTH background. This is consistent with only class C and E *vps* mutants being synthetic lethal in this context, because *vps41* alleles are class B mutations and *vps3* strains are class D. This suggests that, individually, the CORVET and HOPS complexes are nonessential in our adaptor mutant, while the combined dysfunction that occurs in class C mutants leads to inviability.

Similar to the loss of Vps16, we identified the deletion of several ESCRT genes to be synthetic lethal with the 4Δ+ENTH genotype (Figure 4B, Table 1). These were the ESCRT-II complex components, Snf8 and Vps36, and the ESCRT-III factor, Snf7, which aids in membrane invagination through the formation of oligomeric spirals.[47,48] Other ESCRT gene mutations, though not synthetic lethal, produced negative genetic interactions in this context; a synthetic sick phenotype was observed for the disruption of the ESCRT-I complex component, Vps28, and ESCRT-III factor, Vps24 (Figure S2). These sick strains were able to grow slowly on medium with 5-FOA but did not readily sector, likely because of decreased fitness with the loss of plasmid-expressed *ENT1*. Unlike these mutations, the disruption of still other ESCRTs appeared to have no effect on the viability or growth of the reporter cells, as *hse1*Δ, *did2*Δ and *vps20*Δ strains readily sectored and grew in the presence of 5-FOA (Figure S2). Thus, not all ESCRT factors are essential in 4Δ+ENTH, and even removing different members of the ESCRT-III complex produced interactions of varying severity. Together, the results of this genetic interaction mapping reveal that that some, but not all, ESCRT and Vps4 complex components are essential for viability in the endocytic adaptor mutant background.

2.5 | Vps4 is necessary for the viability of an additional endocytosis mutant

We next investigated the possibility that Vps4 may also be essential in other endocytosis mutants. Therefore, we aimed to determine if mutations in End3, a late-coat endocytic protein that acts in conjunction with Pan1 and Sla1,[49,50] are synthetic lethal in a *vps4*Δ strain. Cells that lack End3 exhibit endocytosis defects similar to those observed in the 4Δ+ENTH strain, including nonspecific accumulation of protein cargoes at the PM.[51] We

transformed *end3*Δ mutants with an End3 [Ura3] plasmid and, subsequently, deleted *VPS4* from the genome. Similar to WT cells, the individual *end3*Δ and *vps4*Δ strains grew in the presence of 5-FOA that selected against the End3 cover plasmid (Figure 5A). Conversely, the double mutant did not form colonies. This indicates that cells lacking both End3 and Vps4 are inviable and reveals the existence of negative genetic interactions between *vps4* mutants and multiple genotypes in which CME is disrupted. The high-throughput interactome studies mentioned previously, which identified connections between multiple endocytosis mutants and the loss of Vps4, may not have detected an interaction with *end3* alleles because of a known suppressor mutation in the yeast deletion collection *end3*Δ strain.[52]

In addition to CME, a Rho1-dependent clathrin-independent endocytosis (CIE) pathway exists in budding yeast. To explore whether upregulation of this separate endocytic mechanism can restore viability of an adaptor mutant strain lacking Vps4, we transformed 4Δ+ENTH *vps4*Δ cells, in this case expressing *ENT1* from a *TRP1*-containing plasmid, with either an empty, high-copy *URA3* plasmid or one that includes the *ROM1* gene. Rom1 is a guanine nucleotide exchange factor (GEF) for Rho1 that enhances activity of the CIE pathway when overexpressed.[27] Though cells with high-copy Rom1 produced smaller colonies than the other strains in this experiment, only yeast overexpressing Rom1 were able to lose the Ent1 [Trp1] cover plasmid and grow in the presence of 5-FAA, which selects against the *TRP1* gene (Figure 5B). Additionally, this CIE mechanism is also upregulated in cells provided with osmotic support,[27,53] and we found that 4Δ+ENTH *vps4*Δ+Ent1 [Ade8 Ura3] mutants were able to sector on both rich and 5-FOA-containing media supplemented with sorbitol (Figure S4A). Together, these data demonstrate that increased activity of a yeast CIE pathway can rescue the synthetic lethality between *VPS4* deletion and 4Δ+ENTH mutants.

2.6 | Vps4 activity is required for maintaining the protein composition of the PM

Having confirmed that *VPS4* is essential in the 4Δ+ENTH strain, we aimed to understand the mechanism of this negative genetic interaction; Vps4 acts at endosomes, whereas the endocytic adaptors, Ent1/2 and Yap1801/2, function at the cell surface. Prior studies have reported an increased concentration of cargoes, including Ste3, at the PM when ESCRT complex components are mutated, even though these proteins localize almost exclusively to the cell interior in WT strains.[54,55] Therefore, we examined the localization of Ste3 in live cells after the deletion of *VPS4*.

As described in previous reports, we observed Ste3-GFP primarily in the vacuoles of WT *MATα* cells (Figure 6A); however, in an otherwise WT background, deletion of *VPS4* caused Ste3-GFP to remain at the vacuolar membrane and in neighboring class E compartments that form in the absence of Vps4. Interestingly, we also noticed that a pool of Ste3-GFP accumulated at the PM of *vps4*Δ cells, suggesting that loss of Vps4 increases the concentration of Ste3 at the PM. Quantification of the PM-localized protein showed a significant increase of Ste3-GFP at the surface of *vps4*Δ cells compared to the WT strain (Figure 6B). We also tested cargo trafficking in ESCRT mutants, including cells lacking other synthetic lethal genes, *SNF8* and *VPS36*, and nonsynthetic lethal genes, *HSE1*

and *VPS20*. The loss of Hse1 and Vps20 had no effect (Figure 6A,B). Deletion of the synthetic lethal ESCRT genes led to a subtle increase in Ste3-GFP at the cell surface, but the difference was not statistically significant compared to the WT strain.

Having observed that loss of Vps4 leads to an accumulation of Ste3-GFP at the PM, we also tested the cargoes Mep3, a high-capacity ammonium permease,[53,56] and Ptr2, a di-/tripeptide transporter.[57] As reported previously,[53] Mep3-GFP and Ptr2-GFP localized predominantly to the vacuole in WT cells (Figure 6C–F). In contrast, the PM concentration of both cargoes increased significantly with the deletion of *VPS4*. The vacuole limiting membrane and prevacuolar organelles were not visible in the Mep3-GFP *vps4*Δ cells, perhaps because of the lower expression level of this permease. Nonetheless, multiple cargo proteins concentrate at the cell surface in the absence of Vps4.

We next sought to determine whether activity of the Vps4 large ATPase domain, specifically, is necessary for normal cargo trafficking. We again utilized a $Vps4^{E233Q}$ plasmid, transforming cells expressing GFP fusions of Ste3, Mep3 or Ptr2. As in the *vps4*Δ strains, the cargoes were present at the PM to a greater extent in the $VPS4^{E233Q}$-transformed cells compared to those with vector alone (Figure S4B). The phenotypes were less pronounced for this dominant-negative allele than with deletion of *VPS4*, likely because of incomplete inhibition of the activity of the WT Vps4 present in these cells (Figure S3). Nonetheless, the observable increase in the localization of proteins to the PM demonstrates that activity of the large ATPase domain of Vps4 is necessary for regulating the amount of these cargoes at the cell surface. Additionally, a previous study in which $VPS4^{E233Q}$ was expressed in strains with fluorescently tagged Ste3 also showed an increased concentration of protein at the surface of cells.[58] Combined, the results led us to conclude that the accumulation of cargoes at the PM is a trafficking phenotype associated with the loss of Vps4.

2.7 | Recycling of endocytosed cargoes is increased in *vps4* mutants

Cargo accumulation at the PM in *vps4* mutants may be because of a direct internalization role for Vps4 at the PM of budding yeast or could arise indirectly as a result of increased recycling of endocytosed proteins. In support of the latter possibility, increased recycling of epidermal growth factor receptor has been reported in mammalian cells lacking functional tumor susceptibility gene 101 (TSG101), an ESCRT-I component and orthologue of the yeast gene, *STP22*.[59] To determine if increased recycling of endocytosed proteins is responsible for the elevated cargo concentration observed at cell surfaces in the absence of Vps4, we generated *vps4*Δ *rcy1*Δ double mutant strains expressing Ste3-, Mep3- or Ptr2-GFP. Rcy1 is involved in the recycling of endocytosed proteins, aiding in the return of cargo from endosomes to the PM[60]; because recent reports suggest that yeast is devoid of early endosomes and that the functions of these organelles are instead carried out at the *trans*-Golgi network, this path may in fact be from Golgi to PM.[10]

Similar to results from our prior experiments, more of the fluorescently tagged cargo proteins localized to the PM in the absence of Vps4 relative to WT (Figure 7A,B). Trafficking at the PM in *rcy1*Δ cells appeared similar to the WT strain for Ste3-GFP; however, there was an increase in the concentration of Mep3-GFP and Ptr2-GFP at the surface of cells lacking Rcy1, though not to the extent of *vps4*Δ strains. Thus, the disruption

of this endocytic recycling mechanism also alters the surface concentration of certain cargoes, perhaps in a transporter-specific or strain background-specific manner. Also, none of the cargoes accumulated at the PM in *vps4*Δ *rcy1*Δ cells to the degree observed in the absence of Vps4 alone. Instead, the proteins localized mainly to amorphous compartments within cells, particularly for Ste3-GFP and Ptr2-GFP (Figure 7A; right panels). The finding that cargoes accumulate at the PM in *vps4* mutants, and that this phenotype is abolished by the additional deletion of *RCY1*, suggests that recycling of internalized cargo proteins is increased in response to the loss of Vps4 functioning. In addition to testing the role of Rcy1, we also attempted to generate strains lacking both Vps4 and Drs2. Drs2 is an aminophospholipid translocase that localizes to the *trans*-Golgi, is orthologous to mammalian ATP8A2, and is also involved in endocytic recycling as a physical interactor of Rcy1.[61–63] However, no tetrads produced four viable spores despite seemingly normal tetrad formation and morphology (Figure S5A).

To identify where the protein cargoes accumulate in *vps4*Δ *rcy1*Δ strains, we stained live cells with the lipophilic dye, FM4–64. At the time of imaging, any FM4–64 present in the cell would be trafficked to the vacuole membrane in WT yeast.[64] In WT, *vps4*Δ and *rcy1*Δ cells, FM4–64 localized to the vacuole membrane and, in cells lacking Vps4, to adjacent class E compartments (Figure S5B). Yet, in the *vps4*Δ *rcy1*Δ cells, we observed the dye in amorphous compartments, similar to the localization of cargo proteins in the double mutants. We also treated these cells with a vacuole stain, CMAC-Arg. The dye revealed that the vacuoles in double mutants were fragmented and did not colocalize with Ste3-GFP, confirming that the cargo-containing organelles are not vacuoles (Figure 7C).

We additionally assessed the localization of high-copy Ist1 fused with mCherry compared to Ste3 in the double mutant context. Ist1 is found at late endosomes and is known to interact directly with Vps4.[65] Interestingly, overexpression of Ist1 in the *vps4*Δ *rcy1*Δ strain restored Ste3-GFP localization to the vacuole limiting membrane and class E compartments, similar to a strain lacking only Vps4 (Figure S5C). Ste3-GFP did not colocalize strongly with Ist1-mCherry punctae in the double mutant, suggesting that cargo proteins do not concentrate within late endosomes. Determining where cargo proteins accumulate in *vps4*Δ *rcy1*Δ cells will be an intriguing direction for future research.

2.8 | Cells lacking both Vps4 and Rcy1 exhibit growth defects

We noticed that *vps4*Δ *rcy1*Δ strains grew more slowly than either individual mutant. Consequently, we performed a quantitative assay in which serial cell dilutions were grown on an agar plate. The *vps4*Δ *rcy1*Δ strain grew slower than the WT cells or either single mutant, and a liquid growth assay produced similar results (Figure 8A,B). The growth curves for cells with either individual gene deletion resembled that of the WT strain. However, the delay in the exponential growth phase of *rcy1*Δ cells, as well as the decrease in density of these cells during stationary phase (Figure 8B), was significant (Table S1). In contrast, the double mutant grew drastically slower than all other strains, indicating that the combined loss of Vps4 and Rcy1 negatively affects budding yeast.

Upon observing the slow growth of *vps4*Δ *rcy1*Δ strains, we tested the ability of these cells to grow at high temperatures. WT, *vps4*Δ and *rcy1*Δ cells were viable on rich medium at

both 30 and 37°C (Figure 8C). However, the double mutant strain was temperature-sensitive and unable to grow at the higher temperature. In support of these data demonstrating negative growth phenotypes, one of the previously mentioned high-throughput analyses of the yeast genetic interactome also detected a negative interaction between the combined loss of *VPS4* and *RCY1*.[42] This genetic connection suggests that cells with MVB pathway protein sorting deficiencies become more reliant on the Rcy1-dependent endocytic recycling pathway.

3 | DISCUSSION

The findings presented in this study reveal negative genetic interactions between components of the CME machinery and ESCRT trafficking factors. The synthetic lethality observed for 4Δ+ENTH cells lacking Vps4 was unanticipated; CME adaptors function at the cytoplasmic leaflet of the PM, while Vps4 is best known for acting at the surface of endosomes to complete ESCRT-dependent cargo sorting. Cargoes nonspecifically concentrate at the PM of CME-deficient strains, a phenotype that we also observed in *vps4*Δ cells. Whereas cargo accumulation results from internalization deficiency in 4Δ+ENTH and *end3*Δ strains, it appears the increase in PM cargo concentration that occurs without Vps4 activity is because of increased endocytic recycling in response to MVB pathway disruption. Fluorescent cargoes did not appear to localize strongly to the PM in *vps4*Δ *rcy1*Δ double mutants, supporting the hypothesis that the loss of Vps4 does not directly inhibit endocytosis but, instead, leads to the return of endocytic cargoes to the cell surface.

This rerouting of protein might be related to the failure of vps4 mutants to deliver material to the vacuole lumen for degradation. Because cargo proteins accumulate within prevacuolar organelles and are unable to reach the vacuole interior in vps4Δ cells, it is possible that cargo buildup in these class E compartments leads to the shuttling of internalized protein into endocytic recycling pathways. Under these circumstances, the PM may act as a sink for cargoes that cannot be properly downregulated. The secretion of vacuolar hydrolases, such as CPY, by MVB pathway mutants is consistent with the redirection of cargoes at prevacuolar organelles into this recycling route. Most importantly, the adverse phenotypes associated with a *vps4*Δ *rcy1*Δ strain suggest that endocytic recycling is important for maintaining growth rates when ESCRT trafficking is disrupted.

Our results, along with those from previously published reports, suggest that recycling of endocytosed cargoes is increased in response to the loss of MVB pathway components.[54,55] This includes the increased EGFR recycling to the PM in cancer-predisposed *tsg101* mutants.[59] Interestingly, inactivating mutations in genes for other ESCRTs and Vps4 complex factors, including *VPS4* itself, have also been implicated in several forms of cancer.[66] In contrast to findings that MVB pathway factors are necessary to keep cargoes from being inappropriately recycled, other studies have demonstrated that specific ESCRTs are, instead, directly involved in the return of internalized proteins to the cell surface. These reports show a reduction in endocytic recycling of specific cargoes to the PM in the absence of individual mammalian proteins in the ESCRT-0 and -I complexes, including ALIX, HRS, STAM and even TSG101; however, other work involving *tsg101* mutants did not identify a decrease in cargo recycling.[67–70] The proteins assessed here all exhibited an increased PM

concentration in the absence of Vps4, suggesting that Vps4 is not involved in endocytic recycling like some early-arriving ESCRT factors. Perhaps only early-acting ESCRTs can recognize cargo and be alternatively utilized for recycling, while later-acting ESCRTs and Vps4 complex members are solely involved in targeting proteins for degradation.

Another unanswered question pertains to the localization of cargo in *vps4*Δ *rcy1*Δ strains. These double mutant cells do not exhibit a clear class E *vps* phenotype. Based on our findings, and consistent with the phenotypes of *vps4* mutations, the cargo-containing organelles observed in *vps4*Δ *rcy1*Δ cells are not vacuoles or late endosomes. It is possible that these structures are enlarged early or recycling endosomes, or exaggerated versions of the prevacuolar organelles normally observed in class E mutants. However, if new thinking regarding the yeast endomembrane system is correct in that the *trans*-Golgi supports early and recycling endosome functions,[10] it is possible that they are, instead, expanded *trans*-Golgi networks, especially since prior studies have shown that Rcy1 acts with Drs2 at the Golgi to promote endocytic recycling.[61–63]

Individual loss of Snf7, Snf8 or Vps36 was also lethal in the 4Δ+ENTH strain, confirming that ESCRT-dependent trafficking is essential in endocytic adaptor mutant cells. Nonetheless, genes encoding Vps4 binding partners, including multiple ESCRT-III complex factors, did not exhibit synthetic lethality. Thus, some ESCRTs and Vps4 complex proteins are not essential for the viability of these endocytosis-deficient cells. The finding that some ESCRT-III proteins are essential in the 4Δ+ENTH context, while others appear to have little effect on their growth, may provide insight as to which ESCRTs are most critical for cargo trafficking and sorting under standard conditions. Perhaps residual ESCRT complex activity, even after the loss of specific ESCRTs, such as Vps20, allows for sufficient protein downregulation to support viability, while the absence of others, like Snf8, inhibits ILV formation to an extent that cells cannot tolerate. Variation in such residual MVB pathway activity is one way to explain why some factors are synthetic lethal while others are not. This idea is consistent with the results of early vacuolar protein sorting studies showing differing levels of CPY secretion between class E mutants.[38] Perhaps a threshold activity level exists, and the subtle differences in Ste3-GFP recycling to the PM in synthetic lethal and non-lethal mutants highlight this threshold (Figure 6A,B).

The loss of early-arriving MVB pathway components, such as Hse1, did not affect growth of endocytosis-deficient cells. In fact, of the proteins tested, the ESCRT-II members Snf8 and Vps36 are the first proteins recruited during ESCRT complex assembly that are necessary for viability of the 4Δ+ENTH strain. This may be because of the nature of cargo recognition and transfer between ESCRTs. Cargo proteins are directly bound by ESCRT-0, -I and -II components. If some ESCRT mutations are indeed associated with greater residual protein downregulation, it is possible that targeted cargoes can still be incorporated into forming ILVs even after the loss of individual ESCRT-0 and -I complex members. However, loss or destabilization of cargo-binding ESCRT-II factors may prevent the sufficient movement of protein into endosomal invaginations formed by the ESCRT-III complex, which surrounds previously concentrated cargoes without direct physical interaction.[66,71] We are currently exploring multiple other hypotheses as to the cause of synthetic lethality between Vps4 loss-of-function and the 4Δ+ENTH background. For example, Vps4 has been shown to

regulate sterol synthesis,[72] and it is possible that changes in membrane fluidity affect the viability of adaptor mutant cells. Perhaps higher membrane rigidity in the absence of Vps4 increases the force required to deform the PM, presenting an additional energy barrier to internalization that endocytosis mutants cannot overcome.

The fact that a genetic interaction was also observed between a vps4 allele and the deletion of another CME gene, *END3*, supports the hypothesis that genetic interactions are common between CME mutants and the loss of Vps4. This, combined with the capacity of upregulated Rho1-dependent CIE to rescue 4Δ+ENTH *vps4*Δ cells, suggests that the source of the negative interaction may not be specific to a particular CME mutant, or even a particular endocytic mechanism. Instead, the synthetic lethality may be related to a general inability to maintain cargo concentrations at the PM below a certain threshold. Though cells can withstand the buildup of cargo at the PM that occurs in either a CME-deficient strain or a *vps4* mutant alone, it is possible that the joining of slowed cargo internalization from the cell surface with increased recycling of endocytosed proteins raises cargo concentrations at the cell surface to a level that cannot be tolerated by budding yeast. Perhaps the PM becomes generally overloaded when both endocytosis and ESCRT-dependent trafficking are disrupted, or the PM concentration of specific proteins, such as amino acid transporters, is too high under these conditions. Though cargo overloading at the PM leading to cell inviability has not been reported previously, we may have identified a genetic scenario in which this occurs.

Alternatively, the source of the negative genetic interaction may be because of the accumulation of misfolded proteins at the cell surface. In yeast, the E3 ubiquitin ligase, Rsp5, mediates the downregulation of most cargoes along the endocytic pathway, targeting damaged proteins at the cell surface for internalization via CME.[73–75] After being incorporated into endocytic vesicles and delivered to the early endosome, cargoes are assessed again by another quality control system that also involves Rsp5.[76–78] Yet, neither ubiquitin nor Rsp5 overexpression rescued synthetic lethal cells (unpublished results), suggesting that a concentration increase of misfolded PM proteins is not the cause of this genetic interaction.

One gene corresponding to a non-class E *vps* mutant was also synthetic lethal in our endocytic adaptor mutant strain. VPS16 encodes a subunit of both the class C core vacuole/endosome tethering (CORVET) and HOPS complexes that are necessary for endosome-endosome fusion and late endosome- or vacuole-vacuole fusion, respectively.[44–46] From our data, it appears that only the disruption of both mechanisms produces synthetic lethality, because mutants in which only one complex is nonfunctional are viable (Figure S2). Whether the ultimate cause of this interaction is distinct or somehow related to MVB pathway interruption remains to be uncovered. The absence of well-organized vacuoles in class C *vps* may also reveal the common element making both this group and class E mutants synthetic lethal in 4Δ+ENTH cells; perhaps the source of the negative genetic interactions is related to a challenge in transporting cargo to vacuoles.

A final open question is why Vps4 was identified in our screen as opposed to other ESCRT-related factors. As mentioned previously, Vps4 may be one of only a few components of

the ESCRT-dependent pathway that decreases the efficiency of this trafficking mechanism below a threshold that is essential in the 4Δ+ENTH context. Several other ESCRT-associated mutations caused only synthetic sickness or produced no observable phenotype. In such scenarios, cells would have sectored during our confirmation tests and been removed from further analyses. This may have occurred for *vps24* and *vps20* mutants, for example. It is also possible that mutations in additional ESCRT proteins are represented in other complementation groups for which the causative gene has yet to be identified. The eventual discovery of mutations in other MVB pathway components in these additional groups appears likely, because many of the complementation groups exhibit class E *vps* phenotypes. This work defines a critical relationship between endocytosis and the MVB pathway.

4 | MATERIALS AND METHODS

4.1 | Strains and plasmids

A complete list of strains and plasmids used in this study can be found in Table 2 and Table 3, respectively. Strains were constructed using PCR-based genomic integration, as described previously.[79–80] For genomic integration of GFP, we designed primers using the F2 and R1 plasmid-specific sequences.[79] Transformations were performed according to standard procedures using the lithium acetate method,[81] and integrations were confirmed by colony PCR (unpublished results).

4.2 | Media and growth conditions

Standard yeast extract/peptone medium with 2% dextrose (YPD) was used for growth of yeast under rich conditions. For ammonium-rich conditions or plasmid maintenance, cells were grown in standard yeast nitrogen base (YNB) medium containing 38 mM ammonium sulfate, 2% dextrose, and appropriate amino acids and nutrients. All yeast strains were grown at 30°C unless otherwise indicated. For counter-selection growth assays, cells were grown on minimal agar medium containing 4.31 μM 5-FOA for selection against *URA3* or 3.22 μM 5-FAA for selection against *TRP1*. For growth assays with osmotic support, cells were grown on YPD agar plates supplemented with 1 M sorbitol.

4.3 | Genomic library

The genomic library utilized in this study was generated by cloning of 8–10 kb fragments of genomic DNA from *Saccharomyces cerevisiae* into BamHI/Bgl II digested pRS200 vector.[37]

4.4 | CPY assay

To assess CPY missorting and secretion, cells were streaked on YPD plates, and a nitrocellulose membrane was overlaid directly onto the cells. Following overnight growth, the membrane was lifted from the agar, and the cells were removed by washing with TBST buffer (50 mM Tris, 150 mM NaCl, 0.1% Tween; pH 7.4). The nitrocellulose was then blocked with TBST containing 5% skim milk, and immune-blotted with mouse anti-CPY (1:1000; Molecular Probes) and HRP-conjugated goat anti-mouse secondary (1:5000) antibodies prior to exposure.

4.5 | Live-cell fluorescence microscopy and quantification

In brief, images were obtained at 30°C using an inverted microscope (Axiovert 200; Carl Zeiss) equipped with a Sensicam (Cooke), an X-Cite 120 PC fluorescence illumination system, and a 100×, 1.4 NA Plan-Apochromat objective lens. Cells were placed on uncoated glass slides and covered with a glass coverslip. Within a given experiment, images were acquired using identical conditions, including exposure and binning; subsequently, brightness and contrast adjustments were applied equally to all images. For *N*-(3-Triethylammoniumpropyl)-4-(6-(4-[Diethylamino] Phenyl) Hexatrienyl) Pyridinium Dibromide (FM4–64) staining, cells were incubated with dye for 15 minutes at 30°C before washing with prewarmed media; cells were then incubated for 45 minutes prior to imaging as described previously.[64] For 7-amino-4-chloromethylcoumarin, L-arginine amide (CMAC-Arg; Thermo Fisher Scientific—Yeast Vacuole Marker Sample Kit, Y7531) staining, cells were incubated with the dye for 30 minutes at 30°C before washing with media. Cells were then incubated for 30 minutes prior to imaging as described above.

To quantify the intensity of fluorescent cargo signal at the PM, ImageJ (Version 2.0.0-rc-69/1.52p) was used to subtract the background signal from images and perform the below analyses; for background subtraction, the rolling ball radius was set to 50.0 pixels and none of the additional options were selected. For each cell, the total and intracellular integrated densities were measured, and the intracellular value subtracted from total to determine cargo concentration at the cell surface. This was done for a minimum of 50 cells per condition. A correction for variation in average cell size between strains was also performed; the PM fluorescence intensity value for each mutant cell of a given strain was multiplied by the ratio of the average cell size for that mutant compared to the WT average. The corrected values were then plotted accordingly. Fluorescence intensity measurements were performed for all cells in a minimum of two separate fields per experimental group. Statistical analyses were performed using Prism (GraphPad); either a Welch's unequal variances *t*-test or one-way ANOVA with Tukey's correction was used.

4.6 | Plate reader growth assay

Growth curves were generated using a TECAN Infinite M200 plate reader. Overnight cultures of cells for each strain were diluted to an OD_{600} of 1.0. One mL of YPD was added to three wells of a clear, flat-bottom 24-well plate per strain, and 10 μL of the diluted cultures were then added to the wells. Orbital shaking was used to keep cells in suspension between readings, and readings for each technical replicate were averaged from 25 individual readings per well.

Supplementary Material

Refer to Web version on PubMed Central for supplementary material.

ACKNOWLEDGMENTS

We would like to thank Dr. Carolyn Norris and the students in her 2012–2016 Genetics Lab courses at Johns Hopkins University for their immense contributions to this project. We thank Markus Babst (University of Utah) for the dominant-negative Vps4 and Ist1-mCherry plasmids. We are also grateful to Michael McCaffery and staff of the JHU Integrated Imaging Center, to our neighboring lab headed by Joel Schildbach, to Risheek Chemudupati for

help with graphic design, and to members of the Wendland Lab for helpful discussion and suggestions. Grant MCB 1024818 from the National Science Foundation (NSF) to BW funded this work. KH was supported in part by an NIH T32 Training Grant (T32 007231–37).

Funding information

National Institutes of Health, Grant/Award Number: T32 007231–37; National Science Foundation, Grant/Award Number: MCB 1024818

REFERENCES

1. Kaksonen M, Sun Y, Drubin DG. A pathway for association of receptors, adaptors, and actin during endocytic internalization. Cell. 2003;115(4):475–487. 10.1016/s0092-8674(03)00883-3. [PubMed: 14622601]
2. Kaksonen M, Toret CP, Drubin DG. A modular design for the clathrin- and actin-mediated endocytosis machinery. Cell. 2005;123(2):305–320. 10.1016/j.cell.2005.09.024. [PubMed: 16239147]
3. Taylor MJ, Perrais D, Merrifield CJ. A high precision survey of the molecular dynamics of mammalian clathrin-mediated endocytosis. PLoS Biol. 2011;9:e1000604. 10.1371/journal.pbio.1000604. [PubMed: 21445324]
4. Engqvist-Goldstein AEY, Drubin DG. Actin assembly and endocytosis: from yeast to mammals. Annu Rev Cell Dev Biol. 2003;19:287–332. 10.1146/annurev.cellbio.19.111401.093127. [PubMed: 14570572]
5. Goode BL, Eskin JA, Wendland B. Actin and endocytosis in budding yeast. Genetics. 2015;199(2):315–358. 10.1534/genetics.112.145540. [PubMed: 25657349]
6. Dunn KW, McGraw TE, Maxfield FR. Iterative fractionation of recycling receptors from lysosomally destined ligands in an early sorting endosome. J Cell Biol. 1989;109(6 Pt 2):3303–3314. 10.1083/jcb.109.6.3303. [PubMed: 2600137]
7. Stoorvogel W, Strous GJ, Geuze HJ, Oorschot V, Schwartz AL. Late endosomes derive from early endosomes by maturation. Cell. 1991;65(3):417–427. 10.1016/0092-8674(91)90459-c. [PubMed: 1850321]
8. van der Sluijs P, Hull M, Webster P, Male P, Goud B, Mellman I. The small GTP-binding protein rab4 controls an early sorting event on the endocytic pathway. Cell. 1992;70(5):729–740. 10.1016/0092-8674(92)90307-x. [PubMed: 1516131]
9. Mayor S, Presley JF, Maxfield FR. Sorting of membrane components from endosomes and subsequent recycling to the cell surface occurs by a bulk flow process. J Cell Biol. 1993;121(6):1257–1269. 10.1083/jcb.121.6.1257. [PubMed: 8509447]
10. Day KJ, Casler J, Glick BS. Budding yeast has a minimal endomembrane system. Dev Cell. 2018;44(1):56–72. 10.1016/j.devcel.2017.12.014. [PubMed: 29316441]
11. Felder S, Miller K, Moehren G, Ullrich A, Schlessinger J, Hopkins CR. Kinase activity controls the sorting of the epidermal growth factor receptor within the multivesicular body. Cell. 1990;61(4):623–634. 10.1016/0092-8674(90)90474-s. [PubMed: 2344614]
12. Gruenberg J, Maxfield FR. Membrane transport in the endocytic pathway. Curr Opin Cell Biol. 1995;7(4):552–563. 10.1016/0955-0674(95)80013-1. [PubMed: 7495576]
13. Babst M MVB vesicle formation: ESCRT-dependent, ESCRT-independent and everything in between. Curr Opin Cell Biol. 2011;23(4):452–457. 10.1016/j.ceb.2011.04.008. [PubMed: 21570275]
14. Futter CE, Pearse A, Hewlett LJ, Hopkins CR. Multivesicular endosomes containing internalized EGF-EGF receptor complexes mature and then fuse directly with lysosomes. J Cell Biol. 1996;132(6):1011–1023. 10.1083/jcb.132.6.1011. [PubMed: 8601581]
15. Reider A, Wendland B. Endocytic adaptors—social networking at the plasma membrane. J Cell Sci. 2011;124(Pt 10):1613–1622. 10.1242/jcs.073395. [PubMed: 21536832]
16. de León N, Valdivieso MH. The long life of an endocytic patch that misses AP-2. Curr Genet. 2016;62(4):765–770. 10.1007/s00294-016-0605-3. [PubMed: 27126383]

17. Smith SM, Baker M, Halebian M, Smith CJ. Weak molecular interactions in clathrin-mediated endocytosis. Front Mol Biosci. 2017;4:72. 10.3389/fmolb.2017.00072. [PubMed: 29184887]
18. Aguilar RC, Watson HA, Wendland B. The yeast Epsin Ent1 is recruited to membranes through multiple independent interactions. J Biol Chem. 2003;278(12):10737–10743. 10.1074/jbc.M211622200. [PubMed: 12529323]
19. Maldonado-Báez L, Dores MR, Perkins EM, Drivas TG, Hicke L, Wendland B. Interaction between Epsin/Yap180 adaptors and the scaffolds Ede1/Pan1 is required for endocytosis. Mol Biol Cell. 2008;19(7):2936–2948. 10.1091/mbc.e07-10-1019. [PubMed: 18448668]
20. Benmerah A, Gagnon J, Bègue B, Mégarbané B, Dautry-Varsat A, Cerf-Bensussan N. The tyrosine kinase substrate eps15 is constitutively associated with the plasma membrane adaptor AP-2. J Cell Biol. 1995;131(6 Pt 2):1831–1838. 10.1083/jcb.131.6.1831. [PubMed: 8557749]
21. Wendland B, McCaffery JM, Xiao Q, Emr SD. A novel fluorescence-activated cell sorter-based screen for yeast endocytosis mutants identifies a yeast homologue of mammalian eps15. J Cell Biol. 1996; 135(6 Pt 1):1485–1500. 10.1083/jcb.135.6.1485. [PubMed: 8978817]
22. Salcini AE, Confalonieri S, Doria M, et al. Binding specificity and in vivo targets of the EH domain, a novel protein-protein interaction module. Genes Dev. 1997;11(17):2239–2249. 10.1101/gad.11.17.2239. [PubMed: 9303539]
23. Itoh T, Koshiba S, Kigawa T, Kikuchi A, Yokoyama S, Takenawa T. Role of the ENTH domain in phosphatidylinositol-4,5-bisphosphate binding and endocytosis. Science. 2001;291(5506):1047–1051. 10.1126/science.291.5506.1047. [PubMed: 11161217]
24. Ford MG, Pearse BM, Higgins MK, et al. Simultaneous binding of PtdIns(4,5)P2 and clathrin by AP180 in the nucleation of clathrin lattices on membranes. Science. 2001;291(5506):1051–1055. 10.1126/science.291.5506.1051. [PubMed: 11161218]
25. Wendland B, Steece KE, Emr SD. Yeast epsins contain an essential N-terminal ENTH domain, bind clathrin and are required for endocytosis. EMBO J. 1999;18(16):4383–4393. 10.1093/emboj/18.16.4383. [PubMed: 10449404]
26. Shaw JD, Hama H, Sohrabi F, DeWald DB, Wendland B. PtdIns(3,5) P2 is required for delivery of endocytic cargo into the multivesicular body. Traffic. 2003;4(7):479–490. 10.1034/j.1600-0854.2003.t01-1-00106.x. [PubMed: 12795693]
27. Prosser DC, Drivas TG, Maldonado-Báez L, Wendland B. Existence of a novel clathrin-independent endocytic pathway in yeast that depends on Rho1 and formin. J Cell Biol. 2011;195(4):657–671. 10.1083/jcb.201104045. [PubMed: 22065638]
28. Prosser DC, Pannunzio AE, Brodsky JL, Thorner J, Wendland B, O'Donnell AF. α-Arrestins participate in cargo selection for both clathrin-independent and clathrin-mediated endocytosis. J Cell Sci. 2015;128(22):4220–4234. 10.1242/jcs.175372. [PubMed: 26459639]
29. Robinson JS, Klionsky DJ, Banta LM, Emr SD. Protein sorting in *Saccharomyces cerevisiae*: isolation of mutants defective in the delivery and processing of multiple vacuolar hydrolases. Mol Cell Biol. 1988;8(11):4936–4948. 10.1128/mcb.8.11.4936. [PubMed: 3062374]
30. Rothman JH, Howald I, Stevens TH. Characterization of genes required for protein sorting and vacuolar function in the yeast *Saccharomyces cerevisiae*. EMBO J. 1989;8(7):2057–2065. [PubMed: 2676511]
31. Babst M, Sato TK, Banta LM, Emr SD. Endosomal transport function in yeast requires a novel AAA-type ATPase, Vps4p. EMBO J. 1997;16(8):1820–1831. 10.1093/emboj/16.8.1820. [PubMed: 9155008]
32. Bender A, Pringle JR. Use of a screen for synthetic lethal and multicopy suppressee mutants to identify two new genes involved in morphogenesis in *Saccharomyces cerevisiae*. Mol Cell Biol. 1991;11(3):1295–1305. 10.1128/mcb.11.3.1295. [PubMed: 1996092]
33. Roman H Studies of gene mutation in *Saccharomyces*. Cold Spring Harb Symp Quant Biol. 1956;21:175–185. 10.1101/sqb.1956.021.01.015. [PubMed: 13433590]
34. Dorfman BZ. The isolation of adenylosuccinate synthetase mutants in yeast by selection for constitutive behavior in pigmented strains. Genetics. 1969;61(2):377–389. [PubMed: 5807803]
35. Jones EW, Fink GR. Regulation of amino acid and nucleotide biosynthesis in yeast. The Molecular Biology of the Yeast Saccharomyces: Metabolism and Gene Expression. New York, NY: Cold Spring Harbor Press; 1982:181–299.

36. Boeke JD, Trueheart J, Natsoulis G, Fink GR. 5-Fluoroorotic acid as a selective agent in yeast molecular genetics. Methods Enzymol. 1987;154:164–175. 10.1016/0076-6879(87)54076-9. [PubMed: 3323810]
37. Connelly C, Hieter P. Budding yeast SKP1 encodes an evolutionarily conserved kinetochore protein required for cell cycle progression. Cell. 1996;86(2):275–285. 10.1016/s0092-8674(00)80099-9. [PubMed: 8706132]
38. Raymond CK, Howald-Stevenson I, Vater CA, Stevens TH. Morphological classification of the yeast vacuolar protein sorting mutants: evidence for a prevacuolar compartment in class E vps mutants. Mol Biol Cell. 1992;3(12):1389–1402. 10.1091/mbc.3.12.1389. [PubMed: 1493335]
39. Stuchell-Brereton MD, Skalicky JJ, Kieffer C, Karren MA, Ghaffarian S, Sundquist WI. ESCRT-III recognition by VPS4 ATPases. Nature. 2007;449(7163):740–744. 10.1038/nature06172. [PubMed: 17928862]
40. Babst M, Wendland B, Estepa EJ, Emr SD. The Vps4p AAA ATPase regulates membrane association of a Vps protein complex required for normal endosome function. EMBO J. 1998;17(11):2982–2993. 10.1093/emboj/17.11.2982. [PubMed: 9606181]
41. Costanzo M, Baryshnikova A, Bellay J, et al. The genetic landscape of a cell. Science. 2010;327(5964):425–431. 10.1126/science.1180823. [PubMed: 20093466]
42. Costanzo M, VanderSluis B, Koch EN, et al. A global genetic interaction network maps a wiring diagram of cellular function. Science. 2016;353(6306):aaf1420. 10.1126/science.aaf1420. [PubMed: 27708008]
43. Toyn JH, Gunyuzlu PL, White WH, Thompson LA, Hollis GF. A counterselection for the tryptophan pathway in yeast: 5-fluoroanthranilic acid resistance. Yeast. 2000;16(6):553–560. 10.1002/(SICI)1097-0061(200004)16:6<553::AID-YEA554>3.0.CO;2-7. [PubMed: 10790693]
44. Ungermann C, Price A, Wickner W. A new role for a SNARE protein as a regulator of the Ypt7/Rab-dependent stage of docking. Proc Natl Acad Sci. 2000;97(16):8889–8891. 10.1073/pnas.160269997. [PubMed: 10908678]
45. Seals DF, Eitzen G, Margolis N, Wickner WT, Price A. A Ypt/Rab effector complex containing the Sec1 homolog Vps33p is required for homotypic vacuole fusion. Proc Natl Acad Sci. 2000;97(17):9402–9407. 10.1073/pnas.160269997. [PubMed: 10944212]
46. Peplowska K, Markgraf DF, Ostrowicz CW, Bange G, Ungermann C. The CORVET tethering complex interacts with the yeast Rab5 homolog Vps21 and is involved in endo-lysosomal biogenesis. Dev Cell. 2007;12(5):739–750. 10.1016/j.devcel.2007.03.006. [PubMed: 17488625]
47. Babst M, Katzmann DJ, Estepa-Sabal EJ, Meerloo T, Emr SD. Escrt-III: an endosome-associated heterooligomeric protein complex required for mvb sorting. Dev Cell. 2002;3(2):271–282. 10.1016/s1534-5807(02)00220-4. [PubMed: 12194857]
48. Chiaruttini N, Redondo-Morata L, Colom A, et al. Relaxation of loaded ESCRT-III spiral springs drives membrane deformation. Cell. 2015;163(4):866–879. 10.1016/j.cell.2015.10.017. [PubMed: 26522593]
49. Tang HY, Munn A, Cai M. EH domain proteins Pan1p and End3p are components of a complex that plays a dual role in organization of the cortical actin cytoskeleton and endocytosis in *Saccharomyces cerevisiae*. Mol Cell Biol. 1997;17(8):4294–4304. 10.1128/mcb.17.8.4294. [PubMed: 9234686]
50. Tang HY, Xu J, Cai M. Pan1p, End3p, and S1a1p, three yeast proteins required for normal cortical actin cytoskeleton organization, associate with each other and play essential roles in cell wall morphogenesis. Mol Cell Biol. 2000;20(1):12–25. 10.1128/mcb.20.1.12-25.2000. [PubMed: 10594004]
51. Raths S, Rohrer J, Crausaz F, Riezman H. end3 and end4: two mutants defective in receptor-mediated and fluid-phase endocytosis in *Saccharomyces cerevisiae*. J Cell Biol. 1993;120(1):55–65. 10.1083/jcb.120.1.55. [PubMed: 8380177]
52. Liu K, Hua Z, Nepute JA, Graham TR. Yeast P4-ATPases Drs2p and Dnf1p are essential cargos of the NPFXD/Sla1p endocytic pathway. Mol Biol Cell. 2007;18(2):487–500. 10.1091/mbc.e06-07-0592. [PubMed: 17122361]

53. Apel AR, Hoban K, Chuartzman S, et al. Syp1 regulates the clathrin-mediated and clathrin-independent endocytosis of multiple cargo proteins through a novel sorting motif. Mol Biol Cell. 2017;28(18):2434–2448. 10.1091/mbc.E15-10-0731. [PubMed: 28701344]
54. Davis NG, Horecka JL, Sprague GF Jr. Cis- and trans-acting functions required for endocytosis of the yeast pheromone receptors. J Cell Biol. 1993;122(1):53–65. 10.1083/jcb.122.1.53. [PubMed: 8391002]
55. Amerik AY, Nowak J, Swaminathan S, Hochstrasser M. The Doa4 deubiquitinating enzyme is functionally linked to the vacuolar protein-sorting and endocytic pathways. Mol Biol Cell. 2000;11(10):3365–3380. 10.1091/mbc.11.10.3365. [PubMed: 11029042]
56. Marini AM, Soussi-Boudekou S, Vissers S, Andre B. A family of ammonium transporters in Saccharomyces cerevisiae. Mol Cell Biol. 1997;17(8):4282–4293. 10.1128/mcb.17.8.4282. [PubMed: 9234685]
57. Steiner HY, Song W, Zhang L, Naider F, Becker JM, Stacey G. An Arabidopsis peptide transporter is a member of a new class of membrane transport proteins. Plant Cell. 1994;6(9):1289–1299. 10.1105/tpc.6.9.1289. [PubMed: 7919993]
58. Prosser DC, Whitworth K, Wendland B. Quantitative analysis of endocytosis with cytoplasmic pHluorin chimeras. Traffic. 2010;11(9):1141–1150. 10.1111/j.1600-0854.2010.01088.x. [PubMed: 20626707]
59. Babst M, Odorizzi G, Estepa EJ, Emr SD. Mammalian tumor susceptibility gene 101 (TSG101) and the yeast homologue, Vps23p, both function in late endosomal trafficking. Traffic. 2000;1(3):248–258. 10.1034/j.1600-0854.2000.010307.x. [PubMed: 11208108]
60. Wiederkehr A, Avaro S, Prescianotto-Baschong C, Haguenauer-Tsapis R, Riezman H. The F-box protein Rcy1p is involved in endocytic membrane traffic and recycling out of an early endosome in Saccharomyces cerevisiae. J Cell Biol. 2000;149(2):397–410. 10.1083/jcb.149.2.397. [PubMed: 10769031]
61. Chen CY, Ingram MF, Rosal PH, Graham TR. Role for Drs2p, a P-type ATPase and potential aminophospholipid translocase, in yeast late Golgi function. J Cell Biol. 1999;147(6):1223–1236. 10.1083/jcb.147.6.1223. [PubMed: 10601336]
62. Furuta N, Fujimura-Kamada K, Saito K, Yamamoto T, Tanaka K. Endocytic recycling in yeast is regulated by putative phospholipid translocases and the Ypt31p/32p-Rcy1p pathway. Mol Biol Cell. 2007;18(1):295–312. 10.1091/mbc.e06-05-0461. [PubMed: 17093059]
63. Hanamatsu H, Fujimura-Kamada K, Yamamoto T, Furuta N, Tanaka K. Interaction of the phospholipid flippase Drs2p with the F-box protein Rcy1p plays an important role in early endosome to trans-Golgi network vesicle transport in yeast. J Biochem. 2014;155(1):51–62. 10.1093/jb/mvt094. [PubMed: 24272750]
64. Baggett JJ, Shaw JD, Sciambi CJ, Watson HA, Wendland B. Fluorescent labeling of yeast. Curr Protoc Cell Biol. 2003;20:4.13.1–4.13.28. 10.1002/0471143030.cb0413s20.
65. Rue SM, Mattei S, Saksena S, Emr SD. Novel Ist1-Did2 complex functions at a late step in multivesicular body sorting. Mol Biol Cell. 2008; 19(2):475–484. 10.1091/mbc.E07-07-0694. [PubMed: 18032584]
66. Alfred V, Vaccari T. When membranes need an ESCRT: endosomal sorting and membrane remodelling in health and disease. Swiss Med Wkly. 2016;146:w14347. 10.4414/smw.2016.14347. [PubMed: 27631343]
67. Hanyaloglu AC, McCullagh E, von Zastrow M. Essential role of hrs in a recycling mechanism mediating functional resensitization of cell signaling. EMBO J. 2005;24(13):2265–2283. 10.1038/sj.emboj.7600688. [PubMed: 15944737]
68. Shi A, Pant S, Balklava Z, Chen CC, Figueroa V, Grant BD. A novel requirement for C. elegans Alix/ALX-1 in RME-1-mediated membrane transport. Curr Biol. 2007;17(22):1913–1924. 10.1016/j.cub.2007.10.045. [PubMed: 17997305]
69. Baldys A, Raymond JR. Critical role of ESCRT machinery in EGFR recycling. Biochemistry. 2009;48(40):9321–9323. 10.1021/bi900865u. [PubMed: 19673488]
70. Chanut-Delalande H, Jung AC, Baer MM, Lin L, Payre F, Affolter M. The Hrs/Stam complex acts as a positive and negative regulator of RTK signaling during drosophila development. PLoS One. 2010;5(4):10245. 10.1371/journal.pone.0010245.

71. Williams RL, Urbé S. The emerging shape of the ESCRT machinery. Nat Rev Mol Cell Biol. 2007;8(5):355–368. 10.1038/nrm2162. [PubMed: 17450176]
72. Wang P, Zhang Y, Li H, Chieu HK, Munn AL, Yang H. AAA ATPases regulate membrane association of yeast oxysterol binding proteins and sterol metabolism. EMBO J. 2005;24(17):2989–2999. 10.1038/sj.emboj.7600764. [PubMed: 16096648]
73. Hein C, Springael JY, Volland C, Haguenauer-Tsapis R, André B. NPl1, an essential yeast gene involved in induced degradation of Gap1 and Fur4 permeases, encodes the Rsp5 ubiquitin-protein ligase. Mol Microbiol. 1995;18(1):77–87. 10.1111/j.1365-2958.1995.mmi_18010077.x. [PubMed: 8596462]
74. Wang G, Yang J, Huibregtse JM. Functional domains of the Rsp5 ubiquitin-protein ligase. Mol Cell Biol. 1999;19(1):342–352. 10.1128/mcb.19.1.342. [PubMed: 9858558]
75. Belgareh-Touzé N, Léon S, Erpapazoglou Z, Stawiecka-Mirota M, Urban-Grimal D, Haguenauer-Tsapis R. Versatile role of the yeast ubiquitin ligase Rsp5p in intracellular trafficking. Biochem Soc Trans. 2008;36(Pt 5):791–796. 10.1042/BST0360791. [PubMed: 18793138]
76. Kee Y, Lyon N, Huibregtse JM. The Rsp5 ubiquitin ligase is coupled to and antagonized by the Ubp2 deubiquitinating enzyme. EMBO J. 2005;24(13):2414–2424. 10.1038/sj.emboj.7600710. [PubMed: 15933713]
77. Ren J, Kee Y, Huibregtse JM, Piper RC. Hse1, a component of the yeast Hrs-STAM ubiquitin-sorting complex, associates with ubiquitin peptidases and a ligase to control sorting efficiency into multivesicular bodies. Mol Biol Cell. 2007;18(1):324–335. 10.1091/mbc.e06-06-0557. [PubMed: 17079730]
78. Lam MH, Emili A. Ubp2 regulates Rsp5 ubiquitination activity in vivo and in vitro. PLoS One. 2013;8:e75372. 10.1371/journal.pone.0075372. [PubMed: 24069405]
79. Longtine MS, McKenzie A III, Demarini DJ, et al. Additional modules for versatile and economical PCR-based gene deletion and modification in *Saccharomyces cerevisiae*. Yeast. 1998;14(10):953–961. 10.1002/(SICI)1097-0061(199807)14:10<953::AID-YEA293>3.0.CO;2-U. [PubMed: 9717241]
80. Goldstein AL, McCusker JH. Three new dominant drug resistance cassettes for gene disruption in *Saccharomyces cerevisiae*. Yeast. 1999;15(14):1541–1553. 10.1002/(SICI)1097-0061(199910)15:14<1541::AID-YEA476>3.0.CO;2-K. [PubMed: 10514571]
81. Schiestl RH, Gietz RD. High efficiency transformation of intact yeast cells using single stranded nucleic acids as a carrier. Curr Genet. 1989;16(5–6):339–346. 10.1007/bf00340712. [PubMed: 2692852]
82. Winzeler EA, Shoemaker DD, Astromoff A, et al. Functional characterization of the S. cerevisiae genome by gene deletion and parallel analysis. Science. 1999;285(5429):901–906. 10.1126/science.285.5429.901. [PubMed: 10436161]
83. Cowles CR, Odorizzi G, Payne GS, Emr SD. The AP-3 adaptor complex is essential for cargo-selective transport to the yeast vacuole. Cell. 1997;91(1):109–118. 10.1016/s0092-8674(01)80013-1. [PubMed: 9335339]
84. Ozaki K, Tanaka K, Imamura H, et al. Rom1p and Rom2p are GDP/GTP exchange proteins (GEPs) for the Rho1p small GTP binding protein in Saccharomyces *cerevisiae*. EMBO J. 1996;15(9):2196–2207. [PubMed: 8641285]
85. Dimaano C, Jones CB, Hanono A, Curtiss M, Babst M. Ist1 regulates Vps4 localization and assembly. Mol Biol Cell. 2008;19(2):465–474. 10.1091/mbc.e07-08-0747. [PubMed: 18032582]
86. Xiao J, Xia H, Yoshino-Koh K, Zhou J, Xu Z. Structural characterization of the ATPase reaction cycle of endosomal AAA protein Vps4. J Mol Biol. 2007;374(3):655–670. 10.1016/j.jmb.2007.09.067. [PubMed: 17949747]

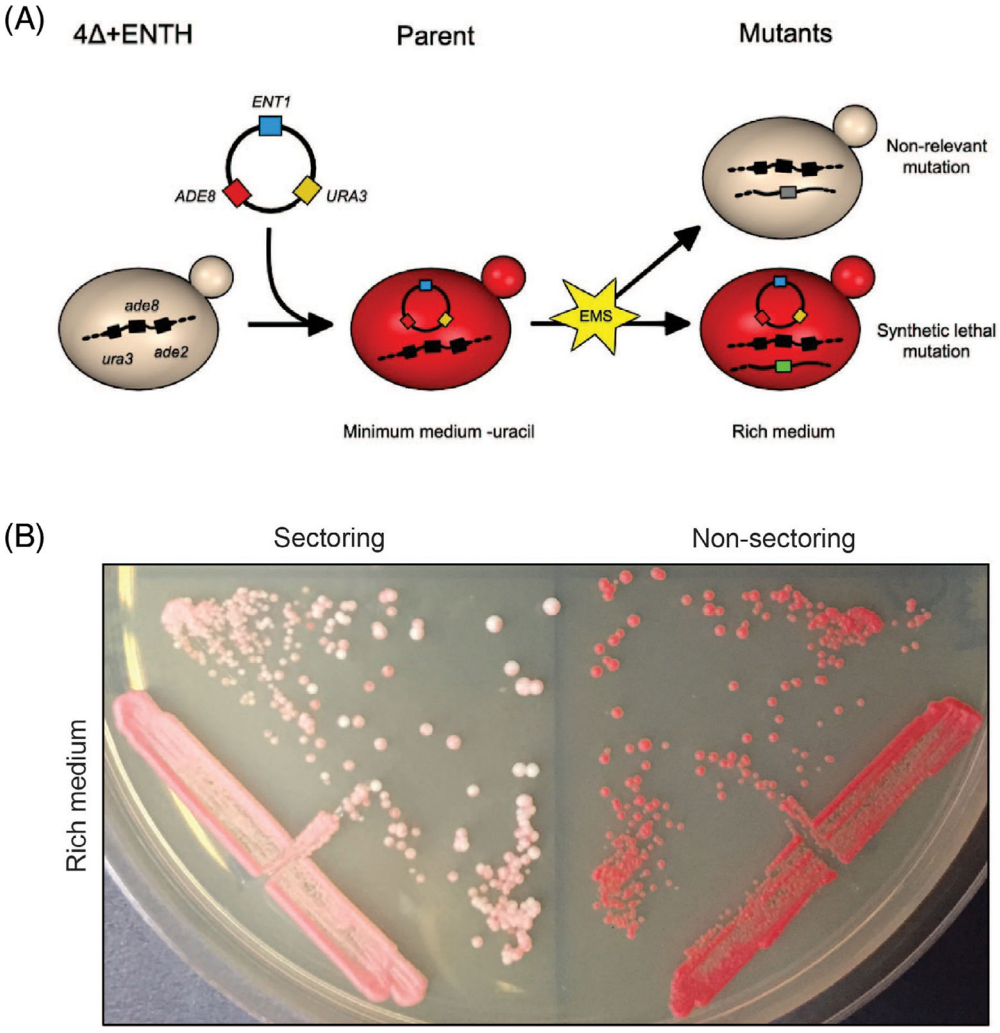

FIGURE 1.

Isolating lethal alleles in cells lacking clathrin-binding adaptors. A, Diagram of mutagenesis and colony-sectoring assay. *ADE2* and *ADE8* were deleted from 4Δ+ENTH cells in which the endogenous *ENT1* locus was truncated immediately after the ENTH domain (4Δ+ENTH *ade2*Δ *ade8*Δ). These cells were transformed with a plasmid containing full-length *ENT1* as well as *ADE8*, resulting in the accumulation of red pigmentation. Following mutagenesis with EMS, cells were plated on rich medium; mutations that do not lead to dependence on full-length Ent1 for viability (gray) will sector upon random loss of this vector during cell division, while synthetic lethal mutations (green) that make cells dependent on the Ent1 plasmid will remain red. B, Cells from a parent strain (4Δ+ENTH+Ent1 [Ade8 Ura3], left) or nonsectoring, synthetic lethal mutant (right) were grown on rich medium. The synthetic lethal mutant requires the Ent1 [Ade8 Ura3] plasmid for viability, producing nonsectoring colonies

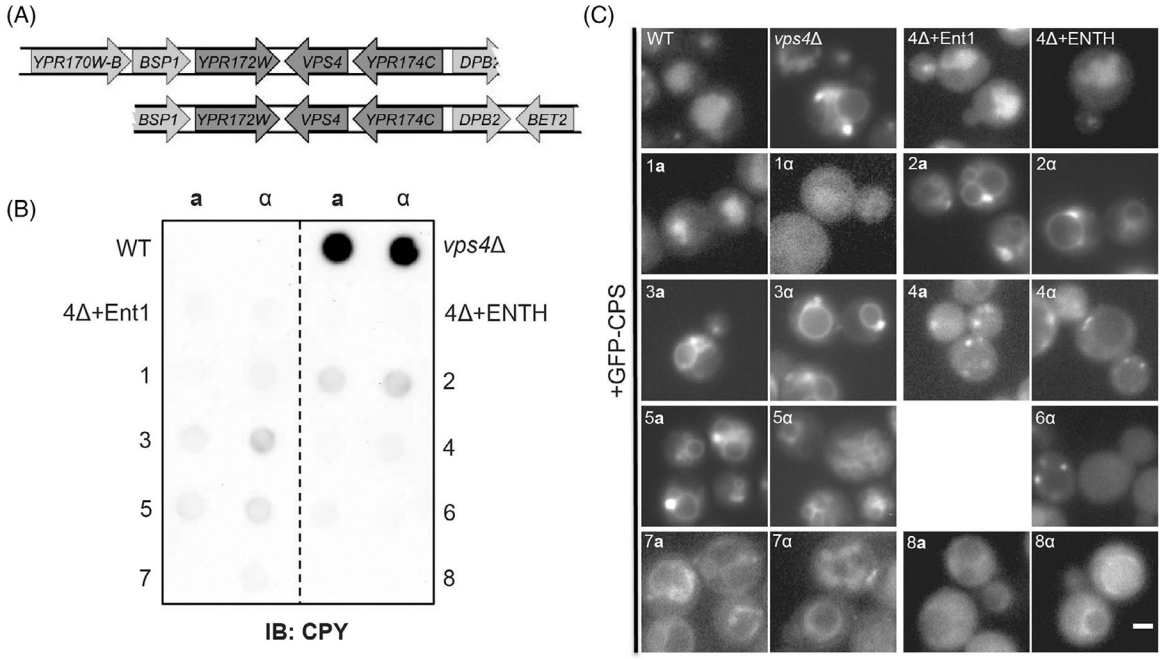

FIGURE 2.

Many synthetic lethal mutants exhibit vacuolar protein sorting defects. A, Graphic illustrating the genomic intervals present on plasmids that rescued mutants from complementation group 3. Genes for which the complete open reading frame was present on both plasmids are indicated in dark gray, while jagged edges and light gray coloring represent genes for which complete open reading frames were present on only one vector. B, CPY secretion assay in which WT, *vps4*Δ, 4Δ+Ent1, 4Δ+ENTH (parent strains) and representative synthetic lethal mutants of both mating types were grown against nitrocellulose and probed with anti-CPY antibodies. All samples were analyzed on the same membrane; the dotted line is used to clarify strain genotype and complementation group locations only. C, Live-cell fluorescence microscopy of WT, *vps4*Δ, 4Δ+Ent1, 4Δ+ENTH (parent strains) and representative synthetic lethal mutant strains transformed with a low-copy GFP-CPS plasmid and grown in minimal medium. The plasmid shuffle necessary for this experiment was unsuccessful for mutant 6**a** even after multiple attempts, likely because of genomic integration of the Ent1 vector. Scale bar, 2 μm

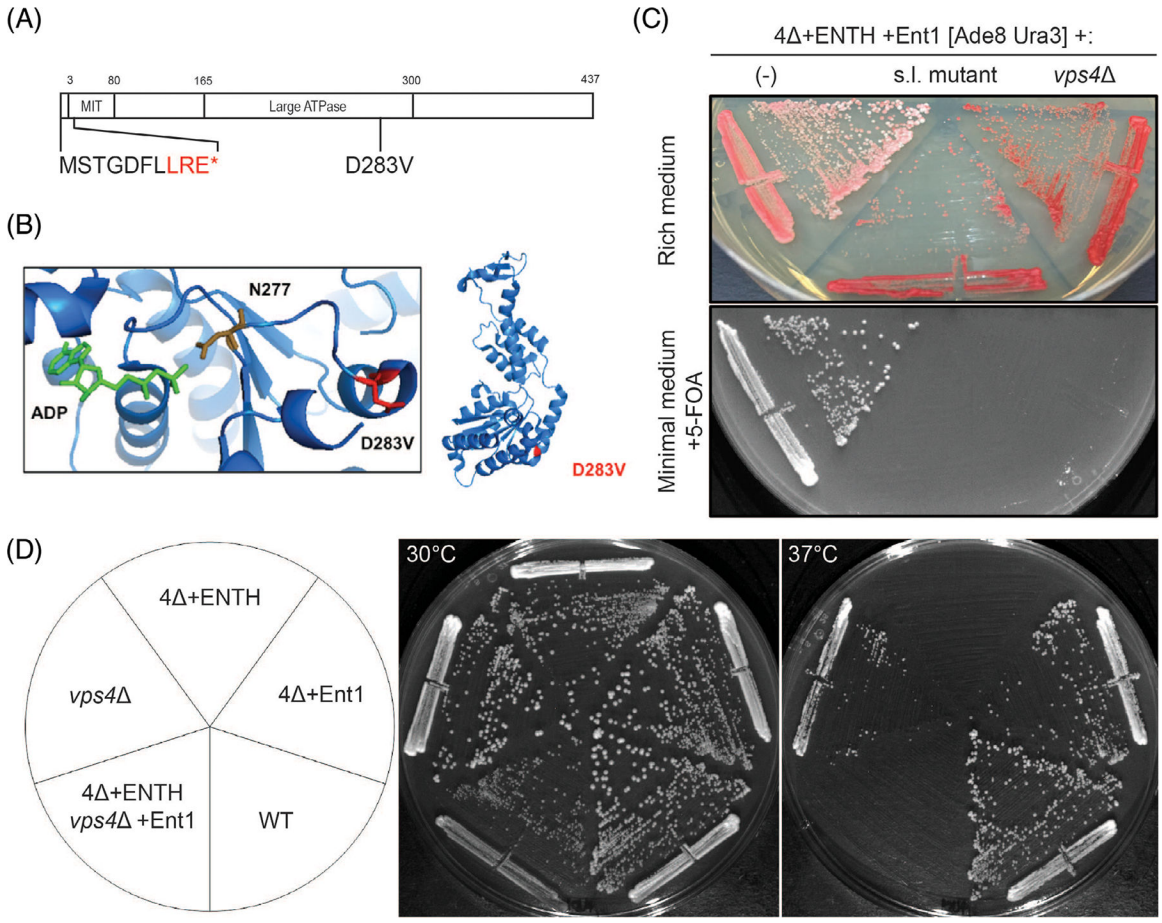

FIGURE 3.

Vps4 mutations are lethal in combination with the 4Δ+ENTH background. A, Diagram of Vps4 in which mutations identified in two representative mutants from complementation group 3 are indicated. The amino acid changes and early stop codon introduced at residue 11 in one of the strains as a result of a frameshift mutation are indicated in red. B, PyMOL-generated depictions of the Vps4 protein.[86] The left image shows the large ATPase domain active site. Residue 283 is highlighted in red, and an ADP molecule within the active site is shown in green. A phosphate-sensing residue, N277, is depicted in brown (The PyMOL Molecular Graphics System, Version 1.8 Schrödinger, LLC). C, Sectoring and growth assays, shown in upper and lower panels, respectively, for a parent strain (4Δ+ENTH+Ent1 [Ade8 Ura3]), a synthetic lethal (s.l.) mutant from complementation group 3, and a parent strain in which *VPS4* was deleted. Cells were tested for sectoring on rich medium and growth on medium containing 5-FOA. D, WT, 4Δ+Ent1, 4Δ+ENTH, *vps4*Δ and 4Δ+ENTH *vps4*Δ+Ent1 strains were grown on rich medium at 30 and 37°C

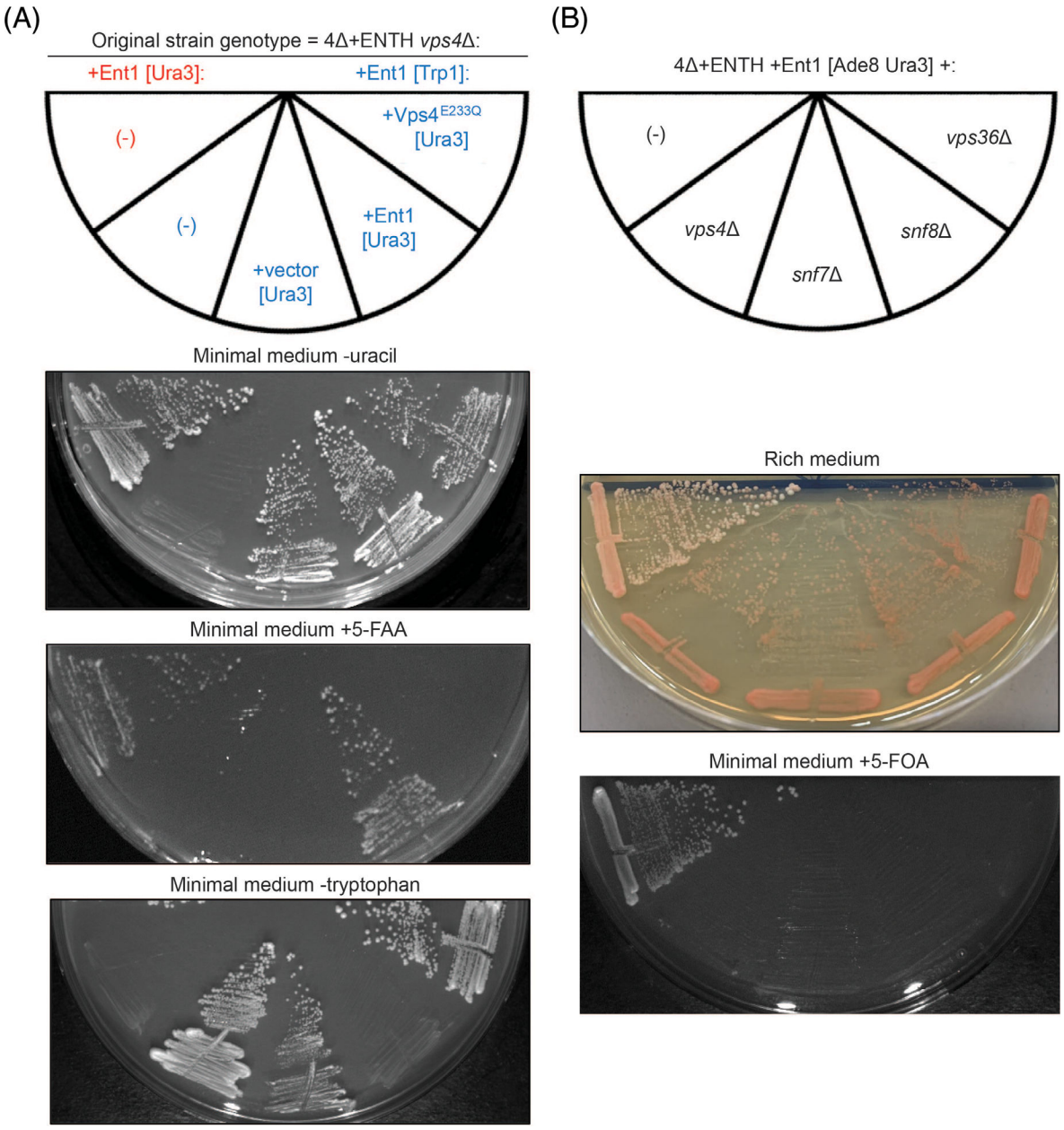

FIGURE 4.

The MVB pathway is essential in 4Δ+ENTH cells. A, Growth assay in which a 4Δ+ENTH *vps4*Δ+Ent1 [Trp1] strain was transformed with a vector expressing *VPS4*^{E233Q} and tested for growth on minimal medium lacking uracil or with 5-FAA. Cells instead transformed with either an empty or Ent1 [Ura3] vector were also included as a negative and positive control for growth on 5-FAA, respectively. Cells that grew on minimal medium+5-FAA were then restreaked onto minimal medium lacking tryptophan to demonstrate that cells no longer possessed the Ent1 [Trp1] plasmid; for scenarios in which cells did not grow in the presence of 5-FAA, original transformants were restreaked. Untransformed strains [(−)] were included as positive and negative controls for growth on the different selection media. Sectors with text in red indicate starting strains with full-length Ent1 on a Ura3 plasmid, while blue

text indicates starting strains with Ent1 on a Trp1 plasmid. B, Sectoring and growth assays shown in upper and lower panels, respectively, for a parent strain (4Δ+ENTH+Ent1 [Ade8 Ura3]), a synthetic lethal *vps4*Δ mutant, and parental strains in which either *SNF7*, *SNF8* or *VPS36* was deleted. Cells were tested for sectoring on rich medium and growth on medium containing 5-FOA

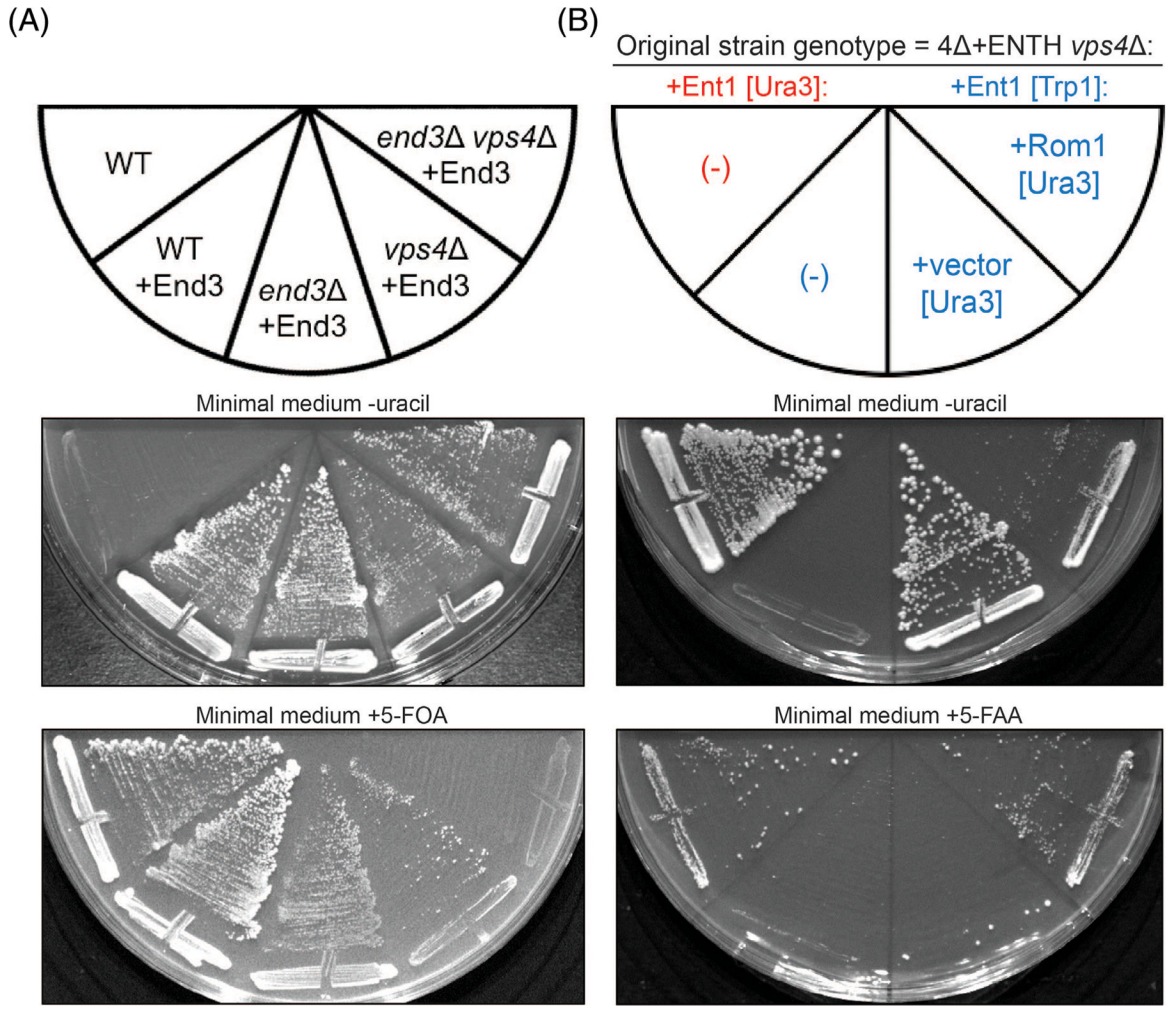

FIGURE 5.

Vps4 is necessary for the viability of an additional endocytosis mutant. A, Growth assay in which WT, *end3*Δ, *vps4*Δ and *end3*Δ *vps4*Δ strains were transformed with an *END3* plasmid also expressing *URA3* and tested for growth on minimal medium lacking uracil or supplemented with 5-FOA, as indicated. Untransformed WT cells were also included as a negative control for growth on medium lacking uracil. B, Growth assay in which a parental strain lacking Vps4 was transformed with either an empty *URA3* vector, or one expressing high-copy Rom1, and tested for growth on minimal medium lacking uracil or containing 5-FAA, as indicated. Untransformed strains [(−)] were included as positive and negative controls for growth. Sectors with text in red indicate starting strains with full-length Ent1 on a Ura3 plasmid, while blue text denotes starting strains with Ent1 on a Trp1 plasmid

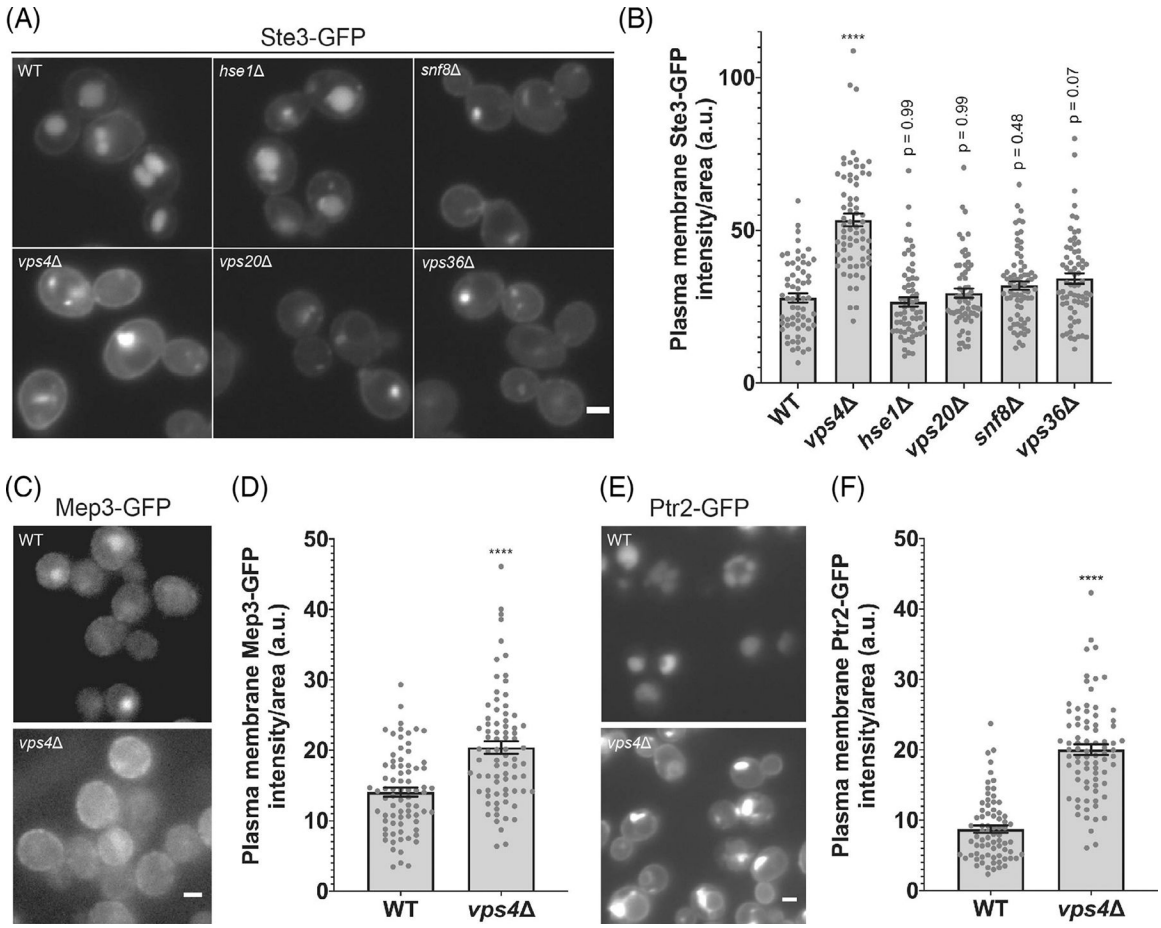

FIGURE 6.

Vps4 activity is required for maintaining the protein composition of the PM. A, Live-cell fluorescence microscopy of WT and MVB pathway mutant strains expressing Ste3-GFP. Scale bar, 2 μm. B, Intensity of Ste3-GFP at the PM was quantified for each condition in A; intensity values were corrected for cell size and expressed in arbitrary units (a.u.). Error bars indicate mean ± SEM; ****, $P < .0001$ compared with WT. C-F, Live-cell fluorescence microscopy of WT and *vps4*Δ strains expressing Mep3- or Ptr2-GFP with quantification of cargo concentration at PM for each strain as in B. Intensity values were corrected for cell size and expressed in arbitrary units (a.u.). Error bars indicate mean ± SEM; ****, $P < .0001$ compared to WT. Scale bars, 2 μm

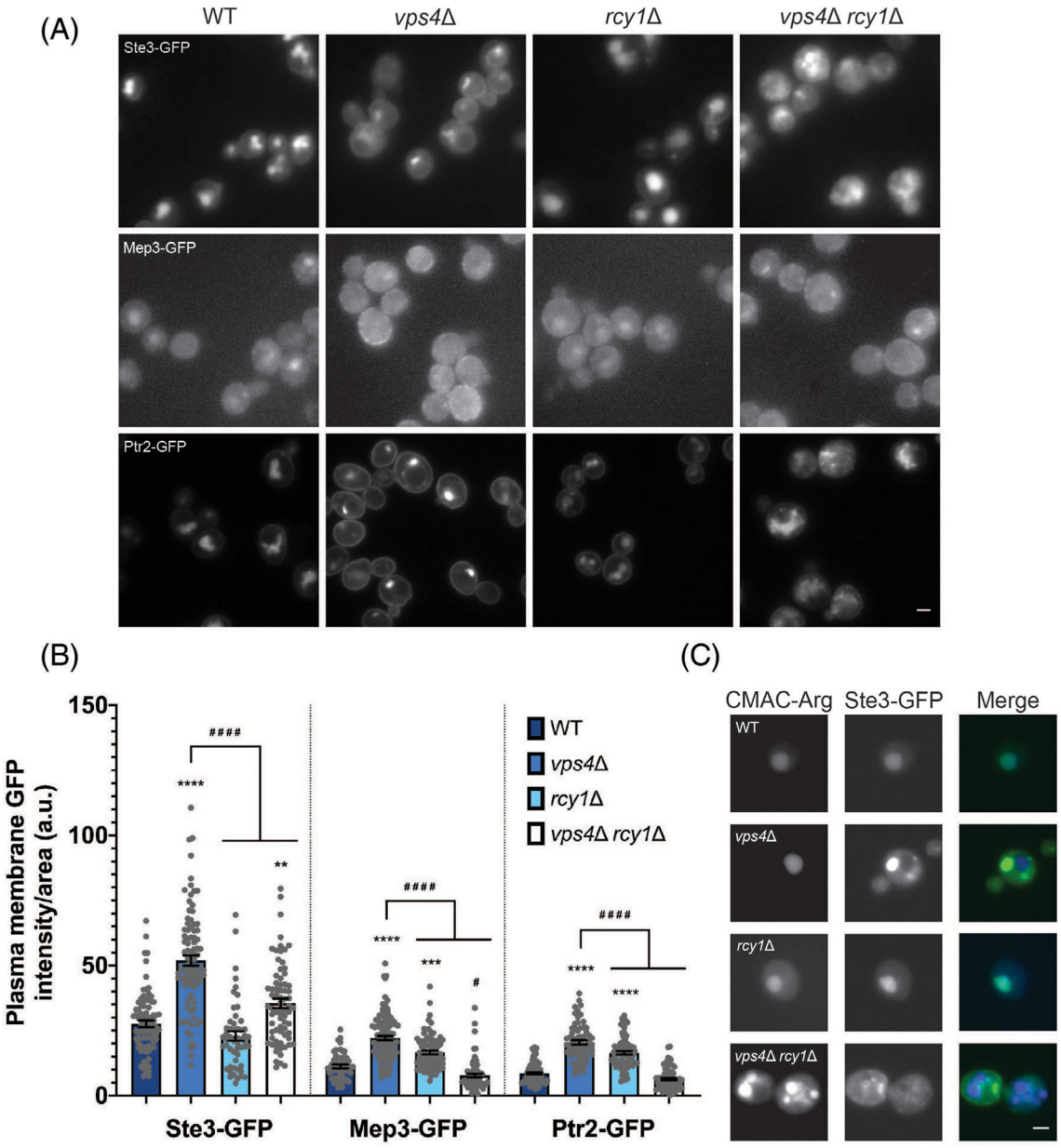

FIGURE 7.

Recycling of endocytosed cargoes is increased in *vps4* mutants. A, Live-cell fluorescence microscopy of Ste3-, Mep3- and Ptr2-GFP localization in WT, *vps4*Δ, *rcy1*Δ, and *vps4*Δ *rcy1*Δ strains grown on rich medium. Scale bar, 2 μm. B, Intensity of fluorescent cargoes at the PM was quantified for each condition; intensity values were corrected for cell size and expressed in arbitrary units (a.u.). Error bars indicate mean ± SEM. Indication of a statistically significant increase compared to WT for a given cargo: ***P* < .01; ****P* < .001; *****P* < .0001. Indication of a statistically significant decrease compared to WT: #, *P* < .05. Indication of a statistically significant decrease compared to *vps4*Δ for a given cargo: ####, *P* < .0001. C, Live-cell fluorescence microscopy of WT, *vps4*Δ, *rcy1*Δ and *vps4*Δ *rcy1*Δ

strains expressing Ste3-GFP incubated in minimal medium with CMAC-Arg stain. Scale bar, 2 μm

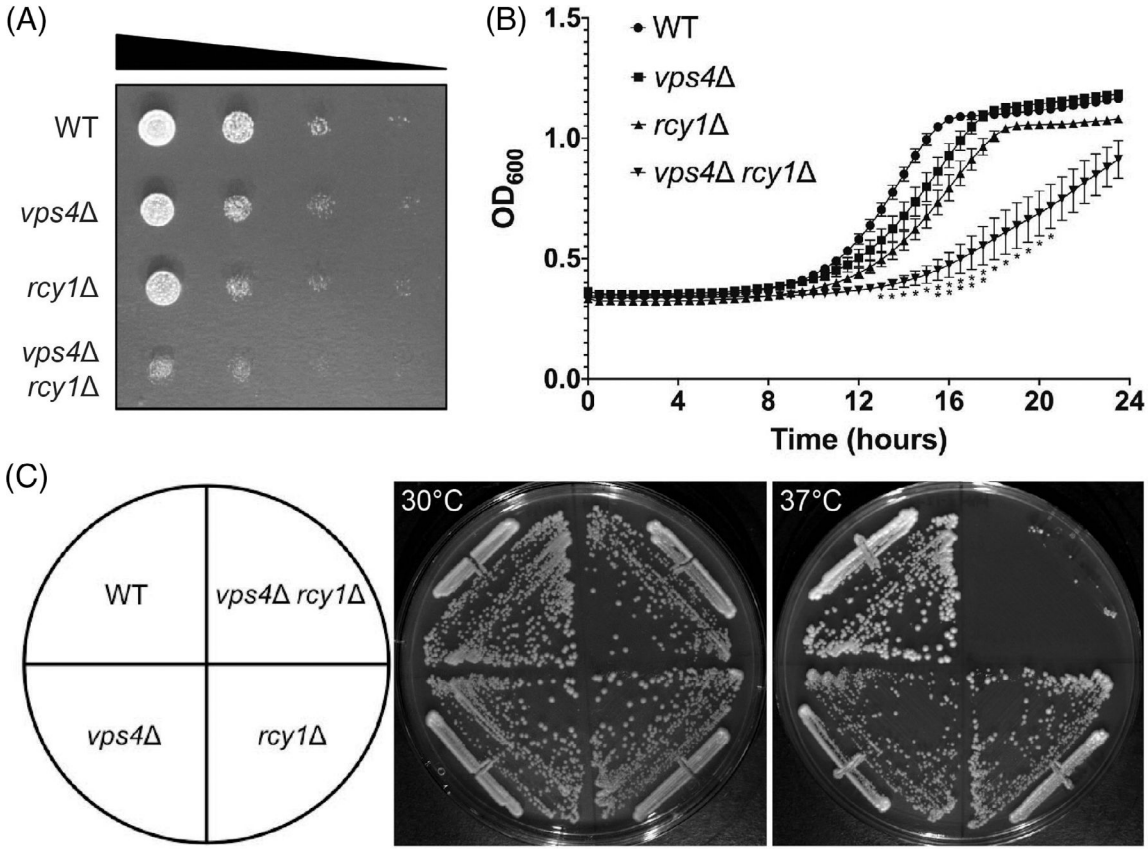

FIGURE 8.

Cells lacking both Vps4 and Rcy1 exhibit growth defects. (A) Plate-based growth assay in which WT, *vps4*Δ, *rcy1*Δ, and *vps4*Δ *rcy1*Δ cells were plated at OD_{600} concentrations of 0.25, 0.05, 0.0025 and 0.0005 OD/mL and grown on rich medium. (B) Liquid culture growth assay in which WT, *vps4*Δ, *rcy1*Δ, or *vps4*Δ *rcy1*Δ cells were grown at the same starting concentration in rich medium for 24 hours. The OD_{600} was measured every 0.5 hours using a TECAN plate reader. Statistically significant differences are only indicated for time points at which *vps4*Δ *rcy1*Δ growth was significantly slower than all other strains (**P* < .05; **, *P* < .01; n = 6). See Table S1 for complete statistical analysis. C, WT, *vps4*Δ, *rcy1*Δ and *vps4*Δ *rcy1*Δ strains were grown on rich medium at 30 and 37°C

TABLE 1

Genes tested for synthetic lethality with 4Δ+ENTH background

Class	Gene	Synthetic lethal?	Increased PM cargo?
A	*PEP1*	No	-
B	*VPS5*	No	-
	VPS41	No	-
C	*VPS16*	Yes	-
D	*VPS3*	No	-
	PEP12	No	-
E; ESCRT-0	*HSE1*	No	No
E; ESCRT-I	*VPS28*	Sick	-
E; ESCRT-II	*SNF8*	Yes	Not significant
	VPS36	Yes	Not significant
E; ESCRT-III and Vps4 Binding Partner	*DID2*	No	-
	SNF7	Yes	-
	VPS20	No	No
	VPS24	Sick	-
E; Vps4 binding partner	*IST1*	No	-
	VFA1	No	-
	VTA1	No	-
E	*VPS4*	Yes	Yes
F	*PEP8*	No	-
Other AAAs	*SAP1*	No	-
	YTA6	No	-

TABLE 2

Strains used in this study

Strain	Genotype	Source
BWY5678	*MAT***a***leu2-3,112 ura3-52 his3-Δ200 trp1-Δ901 suc2-Δ9 lys2-801; GAL ent1::ENTH1::KAN ent2::HIS3 yap1801::HIS3 yap1802::LEU2 ade2::NAT ade8::NAT* +pBW2141	This study
BWY5679	*MAT*α *leu2-3,112 ura3-52 his3-Δ200 trp1-Δ901 suc2-Δ9 lys2-801; GAL ent1::ENTH1::KAN ent2::HIS3 yap1801::HIS3 yap1802::LEU2 ade2::HPH ade8::HPH* +pBW2141	This study
SEY6210	*MAT***a***leu2-3112 ura3-52 his3-Δ200 trp1-Δ901 suc2-Δ9 lys2-801; GAL*	Laboratory strain
BWY6968	*MAT***a***his3Δ1 leu2Δ0 met15Δ0 ura3Δ0 vps4::KAN*	Winzeler et al[82]
BWY2596	*MAT*α *leu2-3,112 ura3-52 his3-Δ200 trp1-Δ901 suc2-Δ9 lys2-801; GAL ent1::LEU2 ent2::HIS3 yap1801::HIS3 yap1802::LEU2* +pBW768	Maldonado-Báez et al[19]
BWY2597	*MAT*α *leu2-3,112 ura3-52 his3-Δ200 trp1-Δ901 suc2-Δ9 lys2-801; GAL ent1::LEU2 ent2::HIS3 yap1801::HIS3 yap1802::LEU2* +pBW778	Maldonado-Báez et al[19]
BWY6684	*MAT*α *leu2-3,112 ura3-52 his3-Δ200 trp1-Δ901 suc2-Δ9 lys2-801; GAL ent1::ENTH1::KAN ent2::HIS3 yap1801::HIS3 yap1802::LEU2 ade2::HPH ade8::HPH vps4::NAT* +pBW2141	This study
BWY6859	*MAT*α *leu2-3112 ura3-52 his3-Δ200 trp1-Δ901 suc2-Δ9 lys2-801; GAL ent1::ENTH1::KAN ent2::HIS3 yap1801::HIS3 yap1802::LEU2 ade2::HPH ade8::HPH vps4::NAT* +pBW308	This study
BWY7146	*MAT*α *leu2-3,112 ura3-52 his3-Δ200 trp1-Δ901 suc2-Δ9 lys2-801; GAL ent1::ENTH1::KAN ent2::HIS3 yap1801::HIS3 yap1802::LEU2 ade2::HPH ade8::HPH snf7::NAT* +pBW2141	This study
BWY7162	*MAT*α *leu2-3,112 ura3-52 his3-Δ200 trp1-Δ901 suc2-Δ9 lys2-801; GAL ent1::ENTH1::KAN ent2::HIS3 yap1801::HIS3 yap1802::LEU2 ade2::HPH ade8::HPH snf8::NAT* +pBW2141	This study
BWY7163	*MAT*α *leu2-3,112 ura3-52 his3-Δ200 trp1-Δ901 suc2-Δ9 lys2-801; GAL ent1::ENTH1::KAN ent2::HIS3 yap1801::HIS3 yap1802::LEU2 ade2::HPH ade8::HPH vps36::NAT* +pBW2141	This study
BWY6949	*MAT*α *leu2-3,112 ura3-52 his3-Δ200 trp1-Δ901 suc2-Δ9 lys2-801; GAL ent1::ENTH1::KAN ent2::HIS3 yap1801::HIS3 yap1802::LEU2 ade2::HPH ade8::HPH vps24::NAT* +pBW2141	This study
BWY6950	*MAT*α *leu2-3,112 ura3-52 his3-Δ200 trp1-Δ901 suc2-Δ9 lys2-801; GAL ent1::ENTH1::KAN ent2::HIS3 yap1801::HIS3 yap1802::LEU2 ade2::HPH ade8::HPH vta1::NAT* +pBW2141	This study
BWY6951	*MAT*α *leu2-3,112 ura3-52 his3-Δ200 trp1-Δ901 suc2-Δ9 lys2-801; GAL ent1::ENTH1::KAN ent2::HIS3 yap1801::HIS3 yap1802::LEU2 ade2::HPH ade8::HPH yta6::NAT* +pBW2141	This study
BWY6952	*MAT*α *leu2-3,112 ura3-52 his3-Δ200 trp1-Δ901 suc2-Δ9 lys2-801; GAL ent1::ENTH1::KAN ent2::HIS3 yap1801::HIS3 yap1802::LEU2 ade2::HPH ade8::HPH vps5::NAT* +pBW2141	This study
BWY7140	*MAT*α *leu2-3,112 ura3-52 his3-Δ200 trp1-Δ901 suc2-Δ9 lys2-801; GAL ent1::ENTH1::KAN ent2::HIS3 yap1801::HIS3 yap1802::LEU2 ade2::HPH ade8::HPH pep12::NAT* +pBW2141	This study
BWY7141	*MAT*α *leu2-3,112 ura3-52 his3-Δ200 trp1-Δ901 suc2-Δ9 lys2-801; GAL ent1::ENTH1::KAN ent2::HIS3 yap1801::HIS3 yap1802::LEU2 ade2::HPH ade8::HPH did2::NAT* +pBW2141	This study
BWY7142	*MAT*α *leu2-3,112 ura3-52 his3-Δ200 trp1-Δ901 suc2-Δ9 lys2-801; GAL ent1::ENTH1::KAN ent2::HIS3 yap1801::HIS3 yap1802::LEU2 ade2::HPH ade8::HPH vps28::NAT* +pBW2141	This study
BWY7143	*MAT*α *leu2-3,112 ura3-52 his3-Δ200 trp1-Δ901 suc2-Δ9 lys2-801; GAL ent1::ENTH1::KAN ent2::HIS3 yap1801::HIS3 yap1802::LEU2 ade2::HPH ade8::HPH sap1::NAT* +pBW2141	This study

Strain	Genotype	Source
BWY7144	*MATα leu2-3,112 ura3-52 his3-Δ200 trp1-Δ901 suc2-Δ9 lys2-801; GAL ent1::ENTH1::KAN ent2::HIS3 yap1801::HIS3 yap1802::LEU2 ade2::HPH ade8::HPH vfa1::NAT* +pBW2141	This study
BWY7145	*MATα leu2-3,112 ura3-52 his3-Δ200 trp1-Δ901 suc2-Δ9 lys2-801; GAL ent1::ENTH1::KAN ent2::HIS3 yap1801::HIS3 yap1802::LEU2 ade2::HPH ade8::HPH pep1::NAT* +pBW2141	This study
BWY7147	*MATα leu2-3,112 ura3-52 his3-Δ200 trp1-Δ901 suc2-Δ9 lys2-801; GAL ent1::ENTH1::KAN ent2::HIS3 yap1801::HIS3 yap1802::LEU2 ade2::HPH ade8::HPH vps20::NAT* +pBW2141	This study
BWY7161	*MATα leu2-3,112 ura3-52 his3-Δ200 trp1-Δ901 suc2-Δ9 lys2-801; GAL ent1::ENTH1::KAN ent2::HIS3 yap1801::HIS3 yap1802::LEU2 ade2::HPH ade8::HPH ist1::NAT* +pBW2141	This study
BWY7164	*MATα leu2-3,112 ura3-52 his3-Δ200 trp1-Δ901 suc2-Δ9 lys2-801; GAL ent1::ENTH1::KAN ent2::HIS3 yap1801::HIS3 yap1802::LEU2 ade2::HPH ade8::HPH pep8::NAT* +pBW2141	This study
BWY7165	*MATα leu2-3,112 ura3-52 his3-Δ200 trp1-Δ901 suc2-Δ9 lys2-801; GAL ent1::ENTH1::KAN ent2::HIS3 yap1801::HIS3 yap1802::LEU2 ade2::HPH ade8::HPH vps16::NAT* +pBW2141	This study
BWY7166	*MATα leu2-3,112 ura3-52 his3-Δ200 trp1-Δ901 suc2-Δ9 lys2-801; GAL ent1::ENTH1::KAN ent2::HIS3 yap1801::HIS3 yap1802::LEU2 ade2::HPH ade8::HPH hse1::NAT* +pBW2141	This study
BWY7184	*MATα leu2-3,112 ura3-52 his3-Δ200 trp1-Δ901 suc2-Δ9 lys2-801; GAL ent1::ENTH1::KAN ent2::HIS3 yap1801::HIS3 yap1802::LEU2 ade2::HPH ade8::HPH vps41::NAT* +pBW2141	This study
BWY7185	*MATα leu2-3,112 ura3-52 his3-Δ200 trp1-Δ901 suc2-Δ9 lys2-801; GAL ent1::ENTH1::KAN ent2::HIS3 yap1801::HIS3 yap1802::LEU2 ade2::HPH ade8::HPH vps3::NAT* +pBW2141	This study
BWY3597	*MATα ura3-1 ade2-1 his3-11 leu2,3112 trp1-1 can1-100 ade2::ADE2 Ste3-GFP::KAN*	Prosser et al[58]
BWY6361	*MATα ura3-1 ade2-1 his3-11 leu2,3112 trp1-1 can1-100 ade2::ADE2 Ste3-GFP::KAN end3::NAT*	This study
BWY4991	*MATa his3Δ1 leu2Δ0 met15Δ0 ura3Δ0 end3::KAN*	This study
BWY5730	*MATa his3Δ1 leu2Δ0 met15Δ0 ura3Δ0 end3::KAN vps4::KAN*	This study
BWY2858	*MATα leu2-3,112 ura3-52 his3-Δ200 trp1-Δ901 suc2-Δ9 lys2-801; GAL Ste3-GFP::KAN*	Prosser et al[28]
BWY7181	*MATα leu2-3,112 ura3-52 his3-Δ200 trp1-Δ901 suc2-Δ9 lys2-801; GAL Ste3-GFP::KAN vps4::NAT*	This study
BWY7178	*MATα leu2-3,112 ura3-52 his3-Δ200 trp1-Δ901 suc2-Δ9 lys2-801; GAL Ste3-GFP::KAN hse1::NAT*	This study
BWY7180	*MATα leu2-3,112 ura3-52 his3-Δ200 trp1-Δ901 suc2-Δ9 lys2-801; GAL Ste3-GFP::KAN vps20::NAT*	This study
BWY7176	*MATα leu2-3,112 ura3-52 his3-Δ200 trp1-Δ901 suc2-Δ9 lys2-801; GAL Ste3-GFP::KAN snf8::NAT*	This study
BWY7177	*MATα leu2-3,112 ura3-52 his3-Δ200 trp1-Δ901 suc2-Δ9 lys2-801; GAL Ste3-GFP::KAN vps36::NAT*	This study
BWY7130	*MATα leu2-3,112 ura3-52 his3-Δ200 trp1-Δ901 suc2-Δ9 lys2-801; GAL Mep3-GFP::KAN*	This study
BWY7131	*MATα leu2-3,112 ura3-52 his3-Δ200 trp1-Δ901 suc2-Δ9 lys2-801; GAL Mep3-GFP::KAN vps4::KAN*	This study
BWY7149	*MATα leu2-3,112 ura3-52 his3-Δ200 trp1-Δ901 suc2-Δ9 lys2-801; GAL Ptr2-GFP::KAN*	This study
BWY7150	*MATα leu2-3,112 ura3-52 his3-Δ200 trp1-Δ901 suc2-Δ9 lys2-801; GAL Ptr2-GFP::KAN vps4::KAN*	This study
BWY6744	*MATα his3Δ1 leu2Δ0 met15Δ0 ura3Δ0 Ste3-GFP::KAN rcy1::KAN*	This study
BWY6743	*MATα his3Δ1 leu2Δ0 met15Δ0 ura3Δ0 Ste3-GFP::KAN vps4::KAN rcyl::KAN*	This study
BWY7134	*MATa leu2-3,112 ura3-52 his3-Δ200 trp1-Δ901 suc2-Δ9 lys2-801; GAL Mep3-GFP::KAN rcy1::KAN*	This study

Strain	Genotype	Source
BWY7135	*MAT***a***leu2-3,112 ura3-52 his3-Δ200 trp1-Δ901 suc2-Δ9 lys2-801; GAL Mep3-GFP::KAN vps4::KAN rcyl::KAN*	This study
BWY7136	*MAT***a***leu2-3,112 ura3-52 his3-Δ200 trp1-Δ901 suc2-Δ9 lys2-801; GAL Ptr2-GFP::KAN rcy1::KAN*	This study
BWY7138	*MAT***a***leu2-3,112 ura3-52 his3-Δ200 trp1-Δ901 suc2-Δ9 lys2-801; GAL Ptr2-GFP::KAN vps4::KAN rcyl::KAN*	This study
BWY6685	*MAT***a***leu2-3,112 ura3-52 his3-Δ200 trp1-Δ901 suc2-Δ9 lys2-801; GAL ent1::ENTH1::KAN ent2::HIS3 yap1801::HIS3 yap1802::LEU2 ade2::NAT ade8::NAT vps4* +pBW2141/ *MATα leu2-3,112 ura3-52 his3-Δ200 trp1-Δ901 suc2-Δ9 lys2-801; GAL ent1::ENTH1::KAN ent2::HIS3 yap1801::HIS3 yap1802::LEU2 ade2::HPH ade8::HPH vps4::NAT* +pBW2141	This study
BWY7154	*MAT***a***his3Δ1 leu2Δ0 met15Δ0 ura3Δ0 drs2::KAN*	Winzeler et al[82]

TABLE 3

Plasmids used in this study

Plasmid	Description	Source
pBW2141	*pRS416::ENT1, pMET-CEN + ADE8*	This study
pBW1063	*pRS416::GFP-CPS*	Cowles et al[83]
pBW308	*pRS414::ENT1*	Baggett et al[64]
pBW768	*pRS414::ENT1*	Maldonado-Báez et al[19]
pBW778	*pRS414::HA-ENTH1*	Baggett et al[64]
pRS416	CEN, *URA3*	Laboratory plasmid
pMB103	*pRS416::vps4*^{E233Q}	Babst et al[31]
pBW910	*pRS416::END3*	This study
pRS426	2 μ, *URA3*	Laboratory plasmid
pBW1622	*pYEP352::ROM1* (2 μ, *URA3*)	Ozaki et al[84]
pMB376	*pRS426::IST1-mCherry*	Dimaano et al[85]